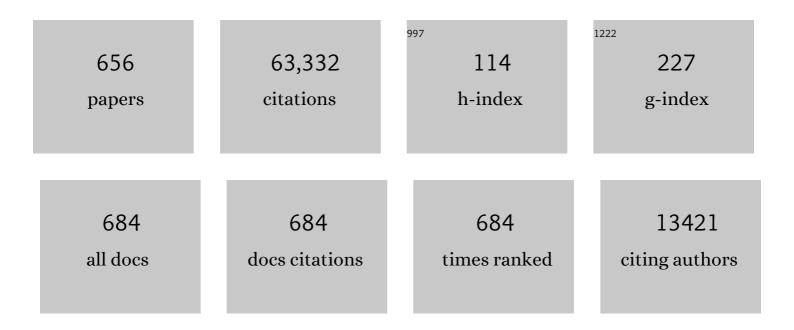
William L. Griffin

List of Publications by Year in descending order

Source: https://exaly.com/author-pdf/2864418/publications.pdf Version: 2024-02-01



#	Article	IF	CITATIONS
1	THREE NATURAL ZIRCON STANDARDS FOR U-TH-PB, LU-HF, TRACE ELEMENT AND REE ANALYSES. Geostandards and Geoanalytical Research, 1995, 19, 1-23.	3.1	4,868
2	The application of laser ablation-inductively coupled plasma-mass spectrometry to in situ U–Pb zircon geochronology. Chemical Geology, 2004, 211, 47-69.	3.3	4,097
3	The Hf isotope composition of cratonic mantle: LAM-MC-ICPMS analysis of zircon megacrysts in kimberlites. Geochimica Et Cosmochimica Acta, 2000, 64, 133-147.	3.9	2,925
4	Zircon chemistry and magma mixing, SE China: In-situ analysis of Hf isotopes, Tonglu and Pingtan igneous complexes. Lithos, 2002, 61, 237-269.	1.4	2,383
5	Igneous zircon: trace element composition as an indicator of source rock type. Contributions To Mineralogy and Petrology, 2002, 143, 602-622.	3.1	2,041
6	Archean crustal evolution in the northern Yilgarn Craton: U–Pb and Hf-isotope evidence from detrital zircons. Precambrian Research, 2004, 131, 231-282.	2.7	983
7	The growth of the continental crust: Constraints from zircon Hf-isotope data. Lithos, 2010, 119, 457-466.	1.4	697
8	Granitoid events in space and time: Constraints from igneous and detrital zircon age spectra. Gondwana Research, 2009, 15, 228-242.	6.0	579
9	Detrital zircon geochronology of Precambrian basement sequences in the Jiangnan orogen: Dating the assembly of the Yangtze and Cathaysia Blocks. Precambrian Research, 2007, 159, 117-131.	2.7	554
10	The Composition and Evolution of Lithospheric Mantle: a Re-evaluation and its Tectonic Implications. Journal of Petrology, 2009, 50, 1185-1204.	2.8	540
11	Phanerozoic evolution of the lithosphere beneath the Sino-Korean craton. Geodynamic Series, 1998, , 107-126.	0.1	524
12	Zircon Crystal Morphology, Trace Element Signatures and Hf Isotope Composition as a Tool for Petrogenetic Modelling: Examples From Eastern Australian Granitoids. Journal of Petrology, 2006, 47, 329-353.	2.8	502
13	Widespread Archean basement beneath the Yangtze craton. Geology, 2006, 34, 417.	4.4	491
14	The lithospheric architecture of Africa: Seismic tomography, mantle petrology, and tectonic evolution. , 2009, 5, 23-50.		477
15	Apatite as an indicator mineral for mineral exploration: trace-element compositions and their relationship to host rock type. Journal of Geochemical Exploration, 2002, 76, 45-69.	3.2	475
16	Application of proton-microprobe data to trace-element partitioning in volcanic rocks. Chemical Geology, 1994, 117, 251-284.	3.3	466
17	The origin and evolution of Archean lithospheric mantle. Precambrian Research, 2003, 127, 19-41.	2.7	432
18	Non-chondritic distribution of the highly siderophile elements in mantle sulphides. Nature, 2000, 407, 891-894.	27.8	428

#	Article	IF	CITATIONS
19	The crust of Cathaysia: Age, assembly and reworking of two terranes. Precambrian Research, 2007, 158, 51-78.	2.7	428
20	SNIP, a statistics-sensitive background treatment for the quantitative analysis of PIXE spectra in geoscience applications. Nuclear Instruments & Methods in Physics Research B, 1988, 34, 396-402.	1.4	394
21	QUANTITATIVE ANALYSIS OF TRACE ELEMENTS IN GEOLOGICAL MATERIALS BY LASER ABLATION ICPMS: INSTRUMENTAL OPERATING CONDITIONS AND CALIBRATION VALUES OF NIST GLASSES. Geostandards and Geoanalytical Research, 1996, 20, 247-261.	3.1	386
22	Components and episodic growth of Precambrian crust in the Cathaysia Block, South China: Evidence from U–Pb ages and Hf isotopes of zircons in Neoproterozoic sediments. Precambrian Research, 2010, 181, 97-114.	2.7	386
23	The density structure of subcontinental lithosphere through time. Earth and Planetary Science Letters, 2001, 184, 605-621.	4.4	382
24	A Paleoproterozoic orogeny recorded in a long-lived cratonic remnant (Wuyishan terrane), eastern Cathaysia Block, China. Precambrian Research, 2009, 174, 347-363.	2.7	374
25	Mesozoic decratonization of the North China block. Geology, 2008, 36, 467.	4.4	341
26	Mechanism and timing of lithospheric modification and replacement beneath the eastern North China Craton: Peridotitic xenoliths from the 100 Ma Fuxin basalts and a regional synthesis. Geochimica Et Cosmochimica Acta, 2007, 71, 5203-5225.	3.9	339
27	Relict refractory mantle beneath the eastern North China block: significance for lithosphere evolution. Lithos, 2001, 57, 43-66.	1.4	328
28	Volatile-bearing minerals and lithophile trace elements in the upper mantle. Chemical Geology, 1997, 141, 153-184.	3.3	307
29	Comment: Hf-isotope heterogeneity in zircon 91500. Chemical Geology, 2006, 233, 358-363.	3.3	297
30	3.6 Ga lower crust in central China: New evidence on the assembly of the North China craton. Geology, 2004, 32, 229.	4.4	295
31	Mantle metasomatism beneath western Victoria, Australia: I. Metasomatic processes in Cr-diopside Iherzolites. Geochimica Et Cosmochimica Acta, 1988, 52, 433-447.	3.9	288
32	Quantitative pixe microanalysis of geological matemal using the CSIRO proton microprobe. Nuclear Instruments & Methods in Physics Research B, 1990, 47, 55-71.	1.4	285
33	Chronology of the pressure-temperature history recorded by a granulite terrain. Contributions To Mineralogy and Petrology, 1988, 98, 303-311.	3.1	282
34	Where was South China in the Rodinia supercontinent?. Precambrian Research, 2008, 164, 1-15.	2.7	281
35	U–Pb geochronology and Hf–Nd isotopic geochemistry of the Badu Complex, Southeastern China: Implications for the Precambrian crustal evolution and paleogeography of the Cathaysia Block. Precambrian Research, 2012, 222-223, 424-449.	2.7	261
36	Geochemical zonation across a Neoproterozoic orogenic belt: Isotopic evidence from granitoids and metasedimentary rocks of the Jiangnan orogen, China. Precambrian Research, 2014, 242, 154-171.	2.7	261

#	Article	IF	CITATIONS
37	Apatite in the mantle: implications for metasomatic processes and high heat production in Phanerozoic mantle. Lithos, 2000, 53, 217-232.	1.4	253
38	Lithospheric, Cratonic, and Geodynamic Setting of Ni-Cu-PGE Sulfide Deposits. Economic Geology, 2010, 105, 1057-1070.	3.8	253
39	U–Pb ages and source composition by Hf-isotope and trace-element analysis of detrital zircons in Permian sandstone and modern sand from southwestern Australia and a review of the paleogeographical and denudational history of the Yilgarn Craton. Earth-Science Reviews, 2005, 68, 245-279.	9.1	250
40	Are Lithospheres Forever? Tracking Changes in Subcontinental Lithospheric Mantle Through Time. GSA Today, 2001, 11, 4.	2.0	242
41	The evolution of lithospheric mantle beneath the Kalahari Craton and its margins. Lithos, 2003, 71, 215-241.	1.4	241
42	Layered Mantle Lithosphere in the Lac de Gras Area, Slave Craton: Composition, Structure and Origin. Journal of Petrology, 1999, 40, 705-727.	2.8	235
43	Harzburgite to lherzolite and back again: metasomatic processes in ultramafic xenoliths from the Wesselton kimberlite, Kimberley, South Africa. Contributions To Mineralogy and Petrology, 1999, 134, 232-250.	3.1	231
44	Continental-root control on the genesis of magmatic ore deposits. Nature Geoscience, 2013, 6, 905-910.	12.9	231
45	A xenolith-derived geotherm for southeastern australia and its geophysical implications. Tectonophysics, 1985, 111, 41-63.	2.2	230
46	Nature and Evolution of Cenozoic Lithospheric Mantle beneath Shandong Peninsula, Sino-Korean Craton, Eastern China. International Geology Review, 1998, 40, 471-499.	2.1	224
47	Apatite Composition: Tracing Petrogenetic Processes in Transhimalayan Granitoids. Journal of Petrology, 2009, 50, 1829-1855.	2.8	223
48	Shear deformation and eclogite formation within granulite-facies anorthosites of the Bergen Arcs, western Norway. Chemical Geology, 1985, 50, 267-281.	3.3	220
49	Genesis of Young Lithospheric Mantle in Southeastern China: an LAM–ICPMS Trace Element Study. Journal of Petrology, 2000, 41, 111-148.	2.8	219
50	Garnet geotherms: Pressure-temperature data from Cr-pyrope garnet xenocrysts in volcanic rocks. Journal of Geophysical Research, 1996, 101, 5611-5625.	3.3	217
51	Precambrian crustal evolution of the Yangtze Block tracked by detrital zircons from Neoproterozoic sedimentary rocks. Precambrian Research, 2010, 177, 131-144.	2.7	215
52	The Siberian lithosphere traverse: mantle terranes and the assembly of the Siberian Craton. Tectonophysics, 1999, 310, 1-35.	2.2	212
53	New insights into the Re–Os systematics of sub-continental lithospheric mantle from in situ analysis of sulphides. Earth and Planetary Science Letters, 2002, 203, 651-663.	4.4	212
54	Tracing Cu and Fe from source to porphyry: in situ determination of Cu and Fe isotope ratios in sulfides from the Grasberg Cu–Au deposit. Chemical Geology, 2004, 207, 147-169.	3.3	210

#	Article	IF	CITATIONS
55	Is the continental Moho the crust-mantle boundary?. Geology, 1987, 15, 241.	4.4	205
56	Thermal and petrological structure of the lithosphere beneath Hannuoba, Sino-Korean Craton, China: evidence from xenoliths. Lithos, 2001, 56, 267-301.	1.4	202
57	Integrated geophysicalâ€petrological modeling of the lithosphere and sublithospheric upper mantle: Methodology and applications. Geochemistry, Geophysics, Geosystems, 2008, 9, .	2.5	200
58	Crustal Evolution in the SW Part of the Baltic Shield: the Hf Isotope Evidence. Journal of Petrology, 2002, 43, 1725-1747.	2.8	198
59	Ultramafic Xenoliths from Bullenmerri and Gnotuk Maars, Victoria, Australia: Petrology of a Sub-Continental Crust-Mantle Transition. Journal of Petrology, 1984, 25, 53-87.	2.8	196
60	Quantitative analysis of trace element abundances in glasses and minerals: a comparison of laser ablation inductively coupled plasma mass spectrometry, solution inductively coupled plasma mass spectrometry, proton microprobe and electron microprobe data. Journal of Analytical Atomic Spectrometry, 1998, 13, 477-482.	3.0	196
61	Superdeep diamonds from the Juina area, Mato Grosso State, Brazil. Contributions To Mineralogy and Petrology, 2001, 140, 734-753.	3.1	195
62	Mineral Chemistry of Peridotites from Paleozoic, Mesozoic and Cenozoic Lithosphere: Constraints on Mantle Evolution beneath Eastern China. Journal of Petrology, 2006, 47, 2233-2256.	2.8	195
63	Triassic "adakitic―rocks in an extensional setting (North China): Melts from the cratonic lower crust. Lithos, 2012, 149, 159-173.	1.4	194
64	Lithosphere mapping beneath the North American plateâ~†. Lithos, 2004, 77, 873-922.	1.4	193
65	In situ Os isotopes in abyssal peridotites bridge the isotopic gap between MORBs and their source mantle. Nature, 2005, 436, 1005-1008.	27.8	190
66	Early crustal evolution in the western Yangtze Block: Evidence from U–Pb and Lu–Hf isotopes on detrital zircons from sedimentary rocks. Precambrian Research, 2012, 222-223, 368-385.	2.7	190
67	The Taihua group on the southern margin of the North China craton: further insights from U–Pb ages and Hf isotope compositions of zircons. Mineralogy and Petrology, 2009, 97, 43-59.	1.1	189
68	U–Pb isotopic ages and Hf isotopic composition of single zircons: The search for juvenile Precambrian continental crust. Precambrian Research, 2005, 139, 42-100.	2.7	187
69	Lithosphere evolution beneath the Kaapvaal Craton: Re–Os systematics of sulfides in mantle-derived peridotites. Chemical Geology, 2004, 208, 89-118.	3.3	186
70	Are continental "adakites―derived from thickened or foundered lower crust?. Earth and Planetary Science Letters, 2015, 419, 125-133.	4.4	176
71	The world turns over: Hadean–Archean crust–mantle evolution. Lithos, 2014, 189, 2-15.	1.4	173
72	In situ measurement of Re-Os isotopes in mantle sulfides by laser ablation multicollector-inductively coupled plasma mass spectrometry: analytical methods and preliminary results. Geochimica Et Cosmochimica Acta, 2002, 66, 1037-1050.	3.9	170

#	Article	IF	CITATIONS
73	Chromitites in ophiolites: How, where, when, why? Part II. The crystallization of chromitites. Lithos, 2014, 189, 140-158.	1.4	170
74	Cadomian (Ediacaran–Cambrian) arc magmatism in the ChahJam–Biarjmand metamorphic complex (Iran): Magmatism along the northern active margin of Gondwana. Gondwana Research, 2015, 27, 439-452.	6.0	170
75	Residence of trace elements in metasomatized spinel lherzolite xenoliths: a proton-microprobe study. Contributions To Mineralogy and Petrology, 1991, 109, 98-113.	3.1	169
76	Caledonian Sm–Nd ages and a crustal origin for Norwegian eclogites. Nature, 1980, 285, 319-321.	27.8	168
77	The trapped fluid phase in upper mantle xenoliths from Victoria, Australia: implications for mantle metasomatism. Contributions To Mineralogy and Petrology, 1984, 88, 72-85.	3.1	168
78	High-Cr and high-Al chromitites from the Sagua de Tánamo district, MayarÃ-Cristal ophiolitic massif (eastern Cuba): Constraints on their origin from mineralogy and geochemistry of chromian spinel and platinum-group elements. Lithos, 2011, 125, 101-121.	1.4	160
79	Archaean and Proterozoic crustal evolution in Lofoten–Vesterålen, N Norway. Journal of the Geological Society, 1978, 135, 629-647.	2.1	159
80	Trace elements in indicator minerals: area selection and target evaluation in diamond exploration. Journal of Geochemical Exploration, 1995, 53, 311-337.	3.2	157
81	Mineral inclusions in diamonds from the Sputnik kimberlite pipe, Yakutia. Lithos, 1997, 39, 135-157.	1.4	156
82	Imaging global chemical and thermal heterogeneity in the subcontinental lithospheric mantle with garnets and xenoliths: Geophysical implications. Tectonophysics, 2006, 416, 289-309.	2.2	151
83	A new model for the evolution of diamond-forming fluids: Evidence from microinclusion-bearing diamonds from Kankan, Guinea. Lithos, 2009, 112, 660-674.	1.4	151
84	Geochronological, geochemical and isotopic study of detrital zircon suites from late Neoproterozoic clastic strata along the NE margin of the East European Craton: Implications for plate tectonic models. Gondwana Research, 2010, 17, 583-601.	6.0	147
85	Granitic magmatism, basement ages, and provenance indicators in the Malay Peninsula: Insights from detrital zircon U–Pb and Hf-isotope data. Gondwana Research, 2011, 19, 1024-1039.	6.0	147
86	Mantle formation and evolution, Slave Craton: constraints from HSE abundances and Re–Os isotope systematics of sulfide inclusions in mantle xenocrysts. Chemical Geology, 2004, 208, 61-88.	3.3	143
87	Trace element composition and cathodoluminescence properties of southern African kimberlitic zircons. Mineralogical Magazine, 1998, 62, 355-366.	1.4	142
88	Mantle metasomatism beneath western Victoria, Australia: II. Isotopic geochemistry of Cr-diopside Iherzolites and Al-augite pyroxenites. Geochimica Et Cosmochimica Acta, 1988, 52, 449-459.	3.9	138
89	Traceâ€element signatures of apatites in granitoids from the Mt Isa Inlier, northwestern Queensland. Australian Journal of Earth Sciences, 2001, 48, 603-619.	1.0	138
90	Early Archaean granulite-facies metamorphism south of Ameralik, West Greenland. Earth and Planetary Science Letters, 1980, 50, 59-74.	4.4	137

#	Article	IF	CITATIONS
91	Mesoarchean subduction processes: 2.87 Ga eclogites from the Kola Peninsula, Russia. Geology, 2010, 38, 739-742.	4.4	137
92	Mantle Recycling: Transition Zone Metamorphism of Tibetan Ophiolitic Peridotites and its Tectonic Implications. Journal of Petrology, 2016, 57, 655-684.	2.8	137
93	Quantitative analysis of PIXE spectra in geoscience applications. Nuclear Instruments & Methods in Physics Research B, 1990, 49, 271-276.	1.4	135
94	Archaean and Proterozoic crustal evolution in the Eastern Succession of the Mt Isa district, Australia: U–ÂPb and Hf-isotope studies of detrital zircons *. Australian Journal of Earth Sciences, 2006, 53, 125-149.	1.0	135
95	Provenance of Lower Cretaceous Wölong Volcaniclastics in the Tibetan Tethyan Himalaya: Implications for the final breakup of Eastern Gondwana. Sedimentary Geology, 2010, 223, 193-205.	2.1	135
96	Mantle Metasomatism. Lecture Notes in Earth System Sciences, 2013, , 471-533.	0.6	135
97	U–Pb and Lu–Hf isotopes in detrital zircon from Neoproterozoic sedimentary rocks in the northern Yangtze Block: Implications for Precambrian crustal evolution. Gondwana Research, 2013, 23, 1261-1272.	6.0	134
98	Multiple events in the Neo-Tethyan oceanic upper mantle: Evidence from Ru–Os–Ir alloys in the Luobusa and Dongqiao ophiolitic podiform chromitites, Tibet. Earth and Planetary Science Letters, 2007, 261, 33-48.	4.4	132
99	Ophiolites of Iran: Keys to understanding the tectonic evolution of SW Asia: (II) Mesozoic ophiolites. Journal of Asian Earth Sciences, 2015, 100, 31-59.	2.3	131
100	Ni in chrome pyrope garnets: a new geothermometer. Contributions To Mineralogy and Petrology, 1989, 103, 199-202.	3.1	130
101	Mapping olivine composition in the lithospheric mantle. Earth and Planetary Science Letters, 2000, 182, 223-235.	4.4	129
102	Mid-Proterozoic magmatic arc evolution at the southwest margin of the Baltic Shieldâ~†. Lithos, 2004, 73, 289-318.	1.4	129
103	Cratonic lithospheric mantle: Is anything subducted?. Episodes, 2007, 30, 43-53.	1.2	129
104	Distribution of K, Rb, Sr and Ba in some minerals relevant to basalt genesis. Geochimica Et Cosmochimica Acta, 1969, 33, 1389-1414.	3.9	125
105	The continental lithosphere–asthenosphere boundary: Can we sample it?. Lithos, 2010, 120, 1-13.	1.4	125
106	Geochemistry and geochronology of Carboniferous volcanic rocks in the eastern Junggar terrane, NW China: Implication for a tectonic transition. Gondwana Research, 2012, 22, 1009-1029.	6.0	124
107	Provenance comparisons of Permian to Jurassic tectonostratigraphic terranes in New Zealand: perspectives from detrital zircon age patterns. Geological Magazine, 2007, 144, 701-729.	1.5	123
108	3â€D multiobservable probabilistic inversion for the compositional and thermal structure of the lithosphere and upper mantle. I: <i>a priori</i> petrological information and geophysical observables. Journal of Geophysical Research: Solid Earth, 2013, 118, 2586-2617.	3.4	121

#	Article	IF	CITATIONS
109	U–Pb and Hf-isotope analysis of zircons in mafic xenoliths from Fuxian kimberlites: evolution of the lower crust beneath the North China craton. Contributions To Mineralogy and Petrology, 2004, 148, 79-103.	3.1	120
110	Mg and Fe-rich carbonate–silicate high-density fluids in cuboid diamonds from the Internationalnaya kimberlite pipe (Yakutia). Lithos, 2009, 112, 638-647.	1.4	120
111	Metasomatism in mantle xenoliths from the Letlhakane kimberlites: estimation of element fluxes. Contributions To Mineralogy and Petrology, 2001, 141, 397-414.	3.1	119
112	Rejuvenation vs. recycling of Archean crust in the Gawler Craton, South Australia: Evidence from U–Pb and Hf isotopes in detrital zircon. Lithos, 2009, 113, 570-582.	1.4	119
113	Re–Os isotopes of sulfides in mantle xenoliths from eastern China: Progressive modification of lithospheric mantle. Lithos, 2008, 102, 43-64.	1.4	117
114	Diachronous decratonization of the Sino-Korean craton: Geochemistry of mantle xenoliths from North Korea. Geology, 2010, 38, 799-802.	4.4	117
115	A xenolith-derived geotherm and the crust-mantle boundary at Qilin, southeastern China. Lithos, 1996, 38, 41-62.	1.4	116
116	Hf contents and Zr/Hf ratios in granitic zircons. Geochemical Journal, 2010, 44, 65-72.	1.0	115
117	Petrological implications of some corona structures. Lithos, 1973, 6, 315-335.	1.4	114
118	Trace-element zoning in garnets from sheared mantle xenoliths. Geochimica Et Cosmochimica Acta, 1989, 53, 561-567.	3.9	114
119	Cr-Pyrope Garnets in the Lithospheric Mantle. I. Compositional Systematics and Relations to Tectonic Setting. Journal of Petrology, 1999, 40, 679-704.	2.8	113
120	Transformation of Archaean Lithospheric Mantle by Refertilization: Evidence from Exposed Peridotites in the Western Gneiss Region, Norway. Journal of Petrology, 2006, 47, 1611-1636.	2.8	113
121	Melt/mantle mixing produces podiform chromite deposits in ophiolites: Implications of Re–Os systematics in the Dongqiao Neo-tethyan ophiolite, northern Tibet. Gondwana Research, 2012, 21, 194-206.	6.0	113
122	Relict Proterozoic basement in the Nanling Mountains (SE China) and its tectonothermal overprinting. Tectonics, 2005, 24, n/a-n/a.	2.8	111
123	Fractionation of oxygen and iron isotopes by partial melting processes: Implications for the interpretation of stable isotope signatures in mafic rocks. Earth and Planetary Science Letters, 2009, 283, 156-166.	4.4	110
124	4-D Lithosphere Mapping: methodology and examples. Tectonophysics, 1996, 262, 3-18.	2.2	109
125	In situ Re-Os analysis of sulfide inclusions in kimberlitic olivine: New constraints on depletion events in the Siberian lithospheric mantle. Geochemistry, Geophysics, Geosystems, 2002, 3, 1-25.	2.5	109
126	Diamond, subcalcic garnet, and mantle metasomatism: Kimberlite sampling patterns define the link. Geology, 2007, 35, 339.	4.4	109

#	Article	IF	CITATIONS
127	Formation history and protolith characteristics of granulite facies metamorphic rock in Central Cathaysia deduced from U-Pb and Lu-Hf isotopic studies of single zircon grains. Science Bulletin, 2005, 50, 2080.	1.7	109
128	Two age populations of zircons from the Timber Creek kimberlites, Northern Territory, as determined by laser-ablation ICP-MS analysis. Australian Journal of Earth Sciences, 2001, 48, 757.	1.0	108
129	Finding of ancient materials in Cathaysia and implication for the formation of Precambrian crust. Science Bulletin, 2007, 52, 13-22.	1.7	108
130	The Pacific Gondwana margin in the late Neoproterozoic–early Paleozoic: Detrital zircon U–Pb ages from metasediments in northwest Argentina reveal their maximum age, provenance and tectonic setting. Gondwana Research, 2011, 19, 71-83.	6.0	108
131	Southward trench migration at â^¼130–120 Ma caused accretion of the Neo-Tethyan forearc lithosphere in Tibetan ophiolites. Earth and Planetary Science Letters, 2016, 438, 57-65.	4.4	108
132	Trace elements in sulfide inclusions from Yakutian diamonds. Contributions To Mineralogy and Petrology, 1996, 124, 111-125.	3.1	107
133	Oxidation during metasomatism in ultramafic xenoliths from the Wesselton kimberlite, South Africa: implications for the survival of diamond. Contributions To Mineralogy and Petrology, 2001, 141, 287-296.	3.1	106
134	Enrichment of upper mantle peridotite: petrological, trace element and isotopic evidence in xenoliths from SE China. Chemical Geology, 2003, 198, 163-188.	3.3	106
135	Linking continental deep subduction with destruction of a cratonic margin: strongly reworked North China SCLM intruded in the Triassic Sulu UHP belt. Contributions To Mineralogy and Petrology, 2014, 168, 1.	3.1	103
136	Trace elements in garnets and chromites: Diamond formation in the Siberian lithosphere. Lithos, 1993, 29, 235-256.	1.4	102
137	Age, geochemistry and tectonic setting of the Neoproterozoic (ca 830Ma) gabbros on the southern margin of the North China Craton. Precambrian Research, 2011, 190, 35-47.	2.7	102
138	Continental crust beneath southeast Iceland. Proceedings of the National Academy of Sciences of the United States of America, 2015, 112, E1818-27.	7.1	102
139	Composition of trapped fluids in cuboid fibrous diamonds from the Udachnaya kimberlite: LAM-ICPMS analysis. Chemical Geology, 2007, 240, 151-162.	3.3	101
140	Ultradeep continental roots and their oceanic remnants: A solution to the geochemical "mantle reservoir―problem?. Lithos, 2009, 112, 1043-1054.	1.4	100
141	Zircons in mantle xenoliths record the Triassic Yangtze–North China continental collision. Earth and Planetary Science Letters, 2006, 247, 130-142.	4.4	99
142	LAM-ICPMS U–Pb dating of kimberlitic perovskite: Eocene–Oligocene kimberlites from the Kundelungu Plateau, D.R. Congo. Earth and Planetary Science Letters, 2008, 267, 609-619.	4.4	99
143	Two age populations of zircons from the Timber Creek kimberlites, Northern Territory, as determined by laser-ablation ICP-MS analysis. Australian Journal of Earth Sciences, 2001, 48, 757-765.	1.0	98
144	Chromitites in ophiolites: How, where, when, why? Part I. A review and new ideas on the origin and significance of platinum-group minerals. Lithos, 2014, 189, 127-139.	1.4	98

#	Article	IF	CITATIONS
145	Ultrapotassic rocks and xenoliths from South Tibet: Contrasting styles of interaction between lithospheric mantle and asthenosphere during continental collision. Geology, 2017, 45, 51-54.	4.4	98
146	Primary sulphide melt inclusions in mantle-derived megacrysts and pyroxenites. Lithos, 1987, 20, 279-294.	1.4	97
147	In-situ U–Pb geochronology and Hf isotope analyses of the Rayner Complex, east Antarctica. Contributions To Mineralogy and Petrology, 2005, 148, 689-706.	3.1	97
148	Accretion and reworking beneath the North China Craton. Lithos, 2012, 149, 61-78.	1.4	97
149	The lower crust and upper mantle beneath northwestern Spitsbergen: evidence from xenoliths and geophysics. Tectonophysics, 1987, 139, 169-185.	2.2	95
150	Archean sulfide inclusions in Paleozoic zircon megacrysts from the Mir kimberlite, Yakutia: implications for the dating of diamonds. Earth and Planetary Science Letters, 2002, 199, 111-126.	4.4	95
151	Screening criteria for reliable U–Pb geochronology and oxygen isotope analysis in uranium-rich zircons: A case study from the Suzhou A-type granites, SE China. Lithos, 2014, 192-195, 180-191.	1.4	95
152	Making it thick: a volcanic plateau origin of Palaeoarchean continental lithosphere of the Pilbara and Kaapvaal cratons. Geological Society Special Publication, 2015, 389, 83-111.	1.3	95
153	Geochemistry and Origin of Sulphide Minerals in Mantle Xenoliths: Qilin, Southeastern China. Journal of Petrology, 1999, 40, 1125-1149.	2.8	94
154	Timing of Late Neoproterozoic glaciation on Baltica constrained by detrital zircon geochronology in the Hedmark Group, south-east Norway. Terra Nova, 2005, 17, 250-258.	2.1	94
155	Tibetan chromitites: Excavating the slab graveyard. Geology, 2015, 43, 179-182.	4.4	94
156	Granulite xenoliths from Cenozoic Basalts in SE China provide geochemical fingerprints to distinguish lower crust terranes from the North and South China tectonic blocks. Lithos, 2003, 67, 77-102.	1.4	92
157	Mineral inclusions and geochemical characteristics of microdiamonds from the DO27, A154, A21, A418, DO18, DD17 and Ranch Lake kimberlites at Lac de Gras, Slave Craton, Canadaâ~†. Lithos, 2004, 77, 39-55.	1.4	92
158	A translithospheric suture in the vanished 1-Ga lithospheric root of South India: Evidence from contrasting lithosphere sections in the Dharwar Craton. Lithos, 2009, 112, 1109-1119.	1.4	91
159	Conditions of diamond growth: a proton microprobe study of inclusions in West Australian diamonds. Contributions To Mineralogy and Petrology, 1988, 99, 143-158.	3.1	90
160	Fingerprints of metamorphism in chromite: New insights from minor and trace elements. Chemical Geology, 2014, 389, 137-152.	3.3	90
161	Variations in trapping temperatures and trace elements in peridotite-suite inclusions from African diamonds: evidence for two inclusion suites, and implications for lithosphere stratigraphy. Contributions To Mineralogy and Petrology, 1992, 110, 1-15.	3.1	89
162	Ophiolites of Iran: Keys to understanding the tectonic evolution of SW Asia: (I) Paleozoic ophiolites. Journal of Asian Earth Sciences, 2014, 91, 19-38.	2.3	87

#	Article	IF	CITATIONS
163	The nature of the Cenozoic lithosphere at Nushan, eastern China. Geodynamic Series, 1998, , 167-195.	0.1	84
164	Sveconorwegian crustal underplating in southwestern Fennoscandia: LAM-ICPMS U–Pb and Lu–Hf isotope evidence from granites and gneisses in Telemark, southern Norway. Lithos, 2007, 93, 273-287.	1.4	84
165	Flood basalts and metallogeny: The lithospheric mantle connection. Earth-Science Reviews, 2008, 86, 145-174.	9.1	84
166	Age and isotopic characterisation of metasedimentary rocks from the Torlesse Supergroup and Waipapa Group in the central North Island, New Zealand. New Zealand Journal of Geology, and Geophysics, 2009, 52, 149-170.	1.8	84
167	Trace element geochemistry of ilmenite megacrysts from the Monastery kimberlite, South Africa. Lithos, 1992, 29, 1-18.	1.4	83
168	Neoproterozoic recycling of the Sveconorwegian orogenic belt: Detrital-zircon data from the Sparagmite basins in the Scandinavian Caledonides. Precambrian Research, 2011, 189, 347-367.	2.7	83
169	Nucleation environment of diamonds from Yakutian kimberlites. Mineralogical Magazine, 1998, 62, 409-419.	1.4	82
170	In-situ hafnium and lead isotope analyses of detrital zircons from the Devonian sedimentary basin of NE Greenland: a record of repeated crustal reworking. Contributions To Mineralogy and Petrology, 2001, 141, 83-94.	3.1	82
171	Reply to "Comment to short-communication ʽComment: Hf-isotope heterogeneity in zircon 91500' by W.L. Griffin, N.J. Pearson, E.A. Belousova and A. Saeed (Chemical Geology 233 (2006) 358–363)―by F. Corfu. Chemical Geology, 2007, 244, 354-356.	3.3	82
172	Nature and timing of metasomatism in the stratified mantle lithosphere beneath the central Slave craton (Canada). Chemical Geology, 2013, 352, 153-169.	3.3	81
173	Secular variation in the composition of subcontinental lithospheric mantle: Geophysical and geodynamic implications. Geodynamic Series, 1998, , 1-26.	0.1	81
174	Nature and evolution of Mesozoic–Cenozoic lithospheric mantle beneath the Cathaysia block, SE China. Lithos, 2004, 74, 41-65.	1.4	80
175	Recycled volatiles determine fertility of porphyry deposits in collisional settings. American Mineralogist, 2021, 106, 656-661.	1.9	80
176	Corundum from basaltic terrains: a mineral inclusion approach to the enigma. Contributions To Mineralogy and Petrology, 1996, 122, 368-386.	3.1	79
177	Zircons in the Shenglikou ultrahigh-pressure garnet peridotite massif and its country rocks from the North Qaidam terrane (western China): Meso-Neoproterozoic crust–mantle coupling and early Paleozoic convergent plate-margin processes. Precambrian Research, 2011, 187, 33-57.	2.7	79
178	Genesis of Coronas in Anorthosites of the Upper Jotun Nappe, Indre Sogn, Norway. Journal of Petrology, 1971, 12, 219-243.	2.8	78
179	A refractory mantle protolith in younger continental crust, east-central China: Age and composition of zircon in the Sulu ultrahigh-pressure peridotite. Geology, 2006, 34, 705.	4.4	78
180	The final stages of kimberlite petrogenesis: Petrography, mineral chemistry, melt inclusions and Sr-C-O isotope geochemistry of the Bultfontein kimberlite (Kimberley, South Africa). Chemical Geology, 2017, 455, 342-356.	3.3	78

#	Article	IF	CITATIONS
181	Ultra-high pressure garnet inclusions in Monastery diamonds: trace element abundance patterns and conditions of origin. European Journal of Mineralogy, 1991, 3, 213-230.	1.3	78
182	Arc-related harzburgite–dunite–chromitite complexes in the mantle section of the Sabzevar ophiolite, Iran: A model for formation of podiform chromitites. Gondwana Research, 2015, 27, 575-593.	6.0	77
183	Neoproterozoic magmatic flare-up along the N. margin of Gondwana: The Taknar complex, NE Iran. Earth and Planetary Science Letters, 2017, 474, 83-96.	4.4	77
184	Zircon inclusions in corundum megacrysts: I. Trace element geochemistry and clues to the origin of corundum megacrysts in alkali basalts. Geochimica Et Cosmochimica Acta, 1996, 60, 2347-2363.	3.9	76
185	Paleozoic diamonds within a Precambrian peridotite lens in UHP gneisses of the Norwegian Caledonides. Earth and Planetary Science Letters, 2002, 203, 805-816.	4.4	76
186	Highly evolved Archean basement beneath the western Cathaysia Block, South China. Geochimica Et Cosmochimica Acta, 2011, 75, 242-255.	3.9	76
187	Emplacement ages and sources of kimberlites and related rocks in southern Africa: U–Pb ages and Sr–Nd isotopes of groundmass perovskite. Contributions To Mineralogy and Petrology, 2014, 168, 1.	3.1	76
188	Minor elements in olivine from spinel lherzolite xenoliths: implications for thermobarometry. Mineralogical Magazine, 1997, 61, 257-269.	1.4	75
189	Quantitative trace-element analysis of diamond by laser ablation inductively coupled plasma mass spectrometry. Journal of Analytical Atomic Spectrometry, 2005, 20, 601.	3.0	74
190	Resetting of the U–Pb Zircon System in Cambro-Ordovician Intrusives of the Deep Freeze Range, Northern Victoria Land, Antarctica. Journal of Petrology, 2007, 48, 327-364.	2.8	74
191	Thermal state and composition of the lithospheric mantle beneath the Daldyn kimberlite field, Yakutia. Tectonophysics, 1996, 262, 19-33.	2.2	73
192	Formation history and protolith characteristics of granulite facies metamorphic rock in Central Cathaysia deduced from U-Pb and Lu-Hf isotopic studies of single zircon grains. Science Bulletin, 2005, 50, 2080-2089.	9.0	73
193	Origin and geological significance of Paleoproterozoic granites in the northeastern Cathaysia Block, South China. Precambrian Research, 2014, 248, 72-95.	2.7	73
194	Inclusions in diamonds from the K14 and K10 kimberlites, Buffalo Hills, Alberta, Canada: diamond growth in a plume?. Lithos, 2004, 77, 99-111.	1.4	72
195	Age and geochemistry of contrasting peridotite types in the Dabie UHP belt, eastern China: Petrogenetic and geodynamic implications. Chemical Geology, 2008, 247, 282-304.	3.3	72
196	Isotopic decoupling during porous melt flow: A case-study in the Lherz peridotite. Earth and Planetary Science Letters, 2009, 279, 76-85.	4.4	72
197	Fibrous diamonds from the placers of the northeastern Siberian Platform: carbonate and silicate crystallization media. Russian Geology and Geophysics, 2011, 52, 1298-1309.	0.7	72
198	Kimberlite genesis from a common carbonate-rich primary melt modified by lithospheric mantle assimilation. Science Advances, 2020, 6, eaaz0424.	10.3	72

#	Article	IF	CITATIONS
199	Subcontinental lithospheric mantle origin of high niobium/tantalum ratios inÂeclogites. Nature Geoscience, 2008, 1, 468-472.	12.9	71
200	Dynamics of cratons in an evolving mantle. Lithos, 2008, 102, 12-24.	1.4	70
201	Heterogeneous and metasomatized mantle recorded by trace elements in minerals of the Donghai garnet peridotites, Sulu UHP terrane, China. Chemical Geology, 2005, 221, 243-259.	3.3	69
202	Sabzevar Ophiolite, NE Iran: Progress from embryonic oceanic lithosphere into magmatic arc constrained by new isotopic and geochemical data. Lithos, 2014, 210-211, 224-241.	1.4	69
203	Plume-subduction interaction forms large auriferous provinces. Nature Communications, 2017, 8, 843.	12.8	69
204	Early Paleozoic tectonic reconstruction of Iran: Tales from detrital zircon geochronology. Lithos, 2017, 268-271, 87-101.	1.4	69
205	Continental collision and accretion recorded in the deep lithosphere of central China. Earth and Planetary Science Letters, 2008, 269, 497-507.	4.4	68
206	On the Vp/Vs–Mg# correlation in mantle peridotites: Implications for the identification of thermal and compositional anomalies in the upper mantle. Earth and Planetary Science Letters, 2010, 289, 606-618.	4.4	68
207	Moho vs crust–mantle boundary: Evolution of an idea. Tectonophysics, 2013, 609, 535-546.	2.2	68
208	The Puncoviscana Formation of northwest Argentina: U-Pb geochronology of detrital zircons and Rb-Sr metamorphic ages and their bearing on its stratigraphic age, sediment provenance and tectonic setting. Neues Jahrbuch Fur Geologie Und Palaontologie - Abhandlungen, 2008, 247, 341-352.	0.4	67
209	3â€D multiobservable probabilistic inversion for the compositional and thermal structure of the lithosphere and upper mantle: III. Thermochemical tomography in the Western entral U.S Journal of Geophysical Research: Solid Earth, 2016, 121, 7337-7370.	3.4	67
210	Trace-element zonation in garnets from The Thumb: heating and melt infiltration below the Colorado Plateau. Contributions To Mineralogy and Petrology, 1991, 107, 60-79.	3.1	66
211	DIAMOND FROM THE GUANIAMO AREA, VENEZUELA. Canadian Mineralogist, 2000, 38, 1347-1370.	1.0	66
212	Tectonic affinity of the west Qinling terrane (central China): North China or Yangtze?. Tectonics, 2010, 29, n/a-n/a.	2.8	66
213	Decoupling of U–Pb and Lu–Hf isotopes and trace elements in zircon from the UHP North Qaidam orogen, NE Tibet (China): Tracing the deep subduction of continental blocks. Lithos, 2012, 155, 125-145.	1.4	66
214	Cenozoic lithospheric architecture and metallogenesis in Southeastern Tibet. Earth-Science Reviews, 2021, 214, 103472.	9.1	66
215	Trace-element partitioning between garnet and clinopyroxene in mantle-derived pyroxenites and eclogites: P-T-X controls. Chemical Geology, 1995, 121, 105-130.	3.3	65
216	The isotopic composition of magnesium in mantle olivine: Records of depletion and metasomatism. Chemical Geology, 2006, 226, 115-133.	3.3	65

#	Article	IF	CITATIONS
217	Early Paleozoic crustal anatexis in the intraplate Wuyi–Yunkai orogen, South China. Lithos, 2013, 175-176, 124-145.	1.4	65
218	Devonian to Permian evolution of the Paleo-Tethys Ocean: New evidence from U–Pb zircon dating and Sr–Nd–Pb isotopes of the Darrehanjir–Mashhad "ophiolites― NE Iran. Gondwana Research, 2015, 28, 781-799.	6.0	65
219	Cu isotopes reveal initial Cu enrichment in sources of giant porphyry deposits in a collisional setting. Geology, 2019, 47, 135-138.	4.4	65
220	Cr-pyrope garnets in the lithospheric mantle 2. Compositional populations and their distribution in time and space. Geochemistry, Geophysics, Geosystems, 2002, 3, 1-35.	2.5	64
221	Type I eclogites from Roberts Victor kimberlites: Products of extensive mantle metasomatism. Geochimica Et Cosmochimica Acta, 2011, 75, 6927-6954.	3.9	64
222	Genesis and tectonic implications of podiform chromitites in the metamorphosed ultramafic massif of Dobromirtsi (Bulgaria). Gondwana Research, 2015, 27, 555-574.	6.0	64
223	Quantitative PIXE microanalysis of fluid inclusions based on a layered yield model. Nuclear Instruments & Methods in Physics Research B, 1991, 54, 292-297.	1.4	63
224	Ghosts of lithospheres past: Imaging an evolving lithospheric mantle in southern Africa. Geology, 2008, 36, 515.	4.4	63
225	Age and composition of granulite and pyroxenite xenoliths in Hannuoba basalts reflect Paleogene underplating beneath the North China Craton. Chemical Geology, 2009, 264, 266-280.	3.3	63
226	Hf isotopes of MARID (mica-amphibole-rutile-ilmenite-diopside) rutile trace metasomatic processes in the lithospheric mantle. Geology, 2005, 33, 45.	4.4	62
227	Crustal Evolution of NW Iran: Cadomian Arcs, Archean Fragments and the Cenozoic Magmatic Flare-Up. Journal of Petrology, 2017, 58, 2143-2190.	2.8	62
228	Scandium speciation in a world-class lateritic deposit. Geochemical Perspectives Letters, 2017, , 105-114.	5.0	62
229	Subduction signature for quenched carbonatites from the deep lithosphere. Geology, 2002, 30, 743.	4.4	61
230	The Evolution of the Upper Mantle beneath the Canary Islands: Information from Trace Elements and Sr isotope Ratios in Minerals in Mantle Xenoliths. Journal of Petrology, 2004, 45, 2573-2612.	2.8	61
231	Neoarchean (2.7–2.8ÂGa) accretion beneath the North China Craton: U–Pb age, trace elements and Hf isotopes of zircons in diamondiferous kimberlites. Lithos, 2009, 112, 188-202.	1.4	61
232	Super-deep diamonds from kimberlites in the Juina area, Mato Grosso State, Brazil. Lithos, 2009, 112, 833-842.	1.4	61
233	High-Mg carbonatitic melts in diamonds, kimberlites and the sub-continental lithosphere. Earth and Planetary Science Letters, 2011, 309, 337-347.	4.4	61
234	H2O contents and their modification in the Cenozoic subcontinental lithospheric mantle beneath the Cathaysia block, SE China. Lithos, 2011, 126, 182-197.	1.4	61

#	Article	IF	CITATIONS
235	Lower-crustal granulites and eclogites from Lesotho, Southern Africa. , 1979, , 59-86.		60
236	The new CSIRO–GEMOC nuclear microprobe: First results, performance and recent applications. Nuclear Instruments & Methods in Physics Research B, 2001, 181, 12-19.	1.4	60
237	Neoproterozoic tonalite and trondhjemite in the Huangling complex, South China: Crustal growth and reworking in a continental arc environment. Numerische Mathematik, 2013, 313, 540-583.	1.4	60
238	The enigma of crustal zircons in upper-mantle rocks: Clues from the Tumut ophiolite, southeast Australia. Geology, 2015, 43, 119-122.	4.4	60
239	The calc-alkaline and adakitic volcanism of the Sabzevar structural zone (NE Iran): Implications for the Eocene magmatic flare-up in Central Iran. Lithos, 2016, 248-251, 517-535.	1.4	60
240	A primitive alkali basaltic stratovolcano and associated eruptive centres, Northwestern Spitsbergen: Volcanology and tectonic significance. Journal of Volcanology and Geothermal Research, 1989, 37, 1-19.	2.1	59
241	Garnetite Xenoliths and Mantle–Water Interactions Below the Colorado Plateau, Southwestern United States. Journal of Petrology, 2005, 46, 1901-1924.	2.8	59
242	Neoproterozoic palaeogeography in the North Atlantic Region: Inferences from the Akkajaure and Seve Nappes of the Scandinavian Caledonides. Precambrian Research, 2011, 186, 127-146.	2.7	59
243	U–Pb zircon ages of Late Cretaceous Nain–Dehshir ophiolites, central Iran. Journal of the Geological Society, 2013, 170, 175-184.	2.1	59
244	Origin of volcanic ash beds across the Permian–Triassic boundary, Daxiakou, South China: Petrology and U–Pb age, trace elements and Hf-isotope composition of zircon. Chemical Geology, 2013, 360-361, 41-53.	3.3	59
245	Genesis and evolution of the lithospheric mantle beneath the Buffalo Head Terrane, Alberta (Canada)â~†. Lithos, 2004, 77, 413-451.	1.4	58
246	Geochronology and provenance of the Late Paleozoic accretionary wedge and Gympie Terrane, New England Orogen, eastern Australiaâ^—. Australian Journal of Earth Sciences, 2009, 56, 655-685.	1.0	58
247	The mantle and crustal evolution of two garnet peridotite suites from the Western Gneiss Region, Norwegian Caledonides: An isotopic investigation. Lithos, 2010, 117, 1-19.	1.4	58
248	μ-FTIR mapping: Distribution of impurities in different types of diamond growth. Diamond and Related Materials, 2012, 29, 29-36.	3.9	58
249	Single zircon LAM-ICPMS U-Pb dating of Guidong complex (SE China) and its petrogenetic significance. Science Bulletin, 2003, 48, 1892-1899.	1.7	57
250	The Kharamai kimberlite field, Siberia: modification of the lithospheric mantle by the Siberian Trap event. Lithos, 2005, 81, 167-187.	1.4	57
251	Thermal and compositional structure of the subcontinental lithospheric mantle: Derivation from shear wave seismic tomography. Geochemistry, Geophysics, Geosystems, 2006, 7, n/a-n/a.	2.5	57
252	Isotopic composition of Mg and Fe in garnet peridotites from the Kaapvaal and Siberian cratons. Geochimica Et Cosmochimica Acta, 2017, 200, 167-185.	3.9	57

#	Article	IF	CITATIONS
253	The flexural rigidity of Fennoscandia: reflection of the tectonothermal age of the lithospheric mantle. Earth and Planetary Science Letters, 1999, 174, 139-154.	4.4	56
254	Lu–Hf and U–Pb isotope systematics of zircons from the Storgangen intrusion, Rogaland Intrusive Complex, SW Norway: implications for the composition and evolution of Precambrian lower crust in the Baltic Shield. Lithos, 2004, 73, 271-288.	1.4	56
255	Melt inclusions from the deep Slave lithosphere: implications for the origin and evolution of mantle-derived carbonatite and kimberlite. Lithos, 2004, 76, 461-474.	1.4	56
256	Comparison between LA-ICP-MS and EPMA analysis of trace elements in diamonds. Chemical Geology, 2008, 252, 158-168.	3.3	56
257	Detrital-zircon ages and geochemistry of sedimentary rocks in basement Mesozoic terranes and their cover rocks in New Caledonia, and provenances at the Eastern Gondwanaland marginâ^—. Australian Journal of Earth Sciences, 2009, 56, 1023-1047.	1.0	56
258	Sulfide and whole rock Re–Os systematics of eclogite and pyroxenite xenoliths from the Slave Craton, Canada. Earth and Planetary Science Letters, 2009, 283, 48-58.	4.4	56
259	Coexisting Early Cretaceous High-Mg Andesites and Adakitic Rocks in the North China Craton: the Role of Water in Intraplate Magmatism and Cratonic Destruction. Journal of Petrology, 2016, 57, 1279-1308.	2.8	56
260	Magmatic evolution of the ultramafic–mafic Kharaelakh intrusion (Siberian Craton, Russia): insights from trace-element, U–Pb and Hf-isotope data on zircon. Contributions To Mineralogy and Petrology, 2010, 159, 753-768.	3.1	54
261	Buoyant ancient continental mantle embedded in oceanic lithosphere (Sal Island, Cape Verde) Tj ETQq1 1 0.78	34314 rgBT 1.4	/Overlock 10
262	Petrogenesis and tectonic implications of Late Carboniferous A-type granites and gabbronorites in NW Iran: Geochronological and geochemical constraints. Lithos, 2015, 212-215, 266-279.	1.4	53
263	Geothermal profile and crust-mantle transition beneath east-central Queensland: Volcanology, xenolith petrology and seismic data. Journal of Volcanology and Geothermal Research, 1987, 31, 177-203.	2.1	52
264	Xenolith geotherms and crustal models in Eastern Australia. Tectonophysics, 1991, 192, 359-366.	2.2	52
265	Taking the pulse of the Earth: linking crustal and mantle events. Australian Journal of Earth Sciences, 2008, 55, 983-995.	1.0	52
266	Sulfides in mantle peridotites from Penghu Islands, Taiwan: Melt percolation, PGE fractionation, and the lithospheric evolution of the South China block. Geochimica Et Cosmochimica Acta, 2009, 73, 4531-4557.	3.9	52
267	Moissanite (SiC) from kimberlites: Polytypes, trace elements, inclusions and speculations on origin. Lithos, 2011, 122, 152-164.	1.4	52
268	First terrestrial occurrence of tistarite (Ti ₂ O ₃): Ultra-low oxygen fugacity in the upper mantle beneath Mount Carmel, Israel. Geology, 2016, 44, 815-818.	4.4	52
269	The nuclear microprobe as a tool in geology and mineral exploration. Nuclear Instruments & Methods in Physics Research B, 1993, 77, 381-398.	1.4	51
270	U-Pb dating of zircons from quartz diorite and its enclaves at Tongguanshan in Anhui and its petrogenetic implication. Science Bulletin, 2004, 49, 2073.	1.7	51

#	Article	IF	CITATIONS
271	Late Mesozoic-Eocene Mantle Replacement beneath the Eastern North China Craton: Evidence from the Paleozoic and Cenozoic Peridotite Xenoliths. International Geology Review, 2005, 47, 457-472.	2.1	51
272	Lithosphere formation in the central Slave Craton (Canada): plume subcretion or lithosphere accretion?. Contributions To Mineralogy and Petrology, 2007, 154, 409-427.	3.1	51
273	U–Pb and Hf isotope data from zircons in the Macquarie Arc, Lachlan Orogen: Implications for arc evolution and Ordovician palaeogeography along part of the east Gondwana margin. Gondwana Research, 2011, 19, 670-685.	6.0	51
274	In situ Re–Os isotopic analysis of platinum-group minerals from the MayarÃ-Cristal ophiolitic massif (MayarÃ-Baracoa Ophiolitic Belt, eastern Cuba): implications for the origin of Os-isotope heterogeneities in podiform chromitites. Contributions To Mineralogy and Petrology, 2011, 161, 977-990.	3.1	51
275	Compositional evolution of high-temperature sheared lherzolite PHN 1611. Geochimica Et Cosmochimica Acta, 1993, 57, 605-613.	3.9	50
276	Alkaline magmatism from Kutch, NW India: implications for plume–lithosphere interaction. Lithos, 2005, 81, 101-119.	1.4	50
277	Recurrent mesoproterozoic continental magmatism in South-Central Norway. International Journal of Earth Sciences, 2009, 98, 1151-1171.	1.8	50
278	Crustal evolution in the central Congo-Kasai Craton, Luebo, D.R. Congo: Insights from zircon U–Pb ages, Hf-isotope and trace-element data. Precambrian Research, 2009, 170, 107-115.	2.7	50
279	Diamonds in ophiolites: Contamination or a new diamond growth environment?. Earth and Planetary Science Letters, 2015, 430, 284-295.	4.4	50
280	Convergent metamorphism of eclogites and dolerites, Kristiansund area, Norway. Lithos, 1973, 6, 21-40.	1.4	49
281	â€~On the eclogites of Norway'—65 years later. Mineralogical Magazine, 1987, 51, 333-343.	1.4	49
282	Diamond-forming fluids in fibrous diamonds: The trace-element perspective. Earth and Planetary Science Letters, 2013, 376, 110-125.	4.4	49
283	Archean mantle fragments in Proterozoic crust, Western Gneiss Region, Norway. Geology, 2004, 32, 609.	4.4	48
284	Trace-element patterns of fibrous and monocrystalline diamonds: Insights into mantle fluids. Lithos, 2010, 118, 313-337.	1.4	48
285	Multi-stage origin of Roberts Victor eclogites: Progressive metasomatism and its isotopic effects. Lithos, 2012, 142-143, 161-181.	1.4	48
286	Pyroxenite Dykes in Orogenic Peridotite from North Qaidam (NE Tibet, China) Track Metasomatism and Segregation in the Mantle Wedge. Journal of Petrology, 2014, 55, 2347-2376.	2.8	48
287	REE, Rbî—,Sr and Smî—,Nd studies of Norwegian eclogites. Chemical Geology: Isotope Geoscience Section, 1985, 52, 249-271.	0.6	47
288	Zoning in eclogite garnets from Nordfjord, West Norway. Contributions To Mineralogy and Petrology, 1971, 32, 112-125.	3.1	46

#	Article	IF	CITATIONS
289	Grenvillian orogeny in the Southern Cathaysia Block: Constraints from U-Pb ages and Lu-Hf isotopes in zircon from metamorphic basement. Science Bulletin, 2008, 53, 3037-3050.	9.0	46
290	Petrogenesis and geochronology of Cretaceous adakitic, I- and A-type granitoids in the NE Yangtze block: Constraints on the eastern subsurface boundary between the North and South China blocks. Lithos, 2013, 175-176, 333-350.	1.4	46
291	Primitive Arc Magmatism and Delamination: Petrology and Geochemistry of Pyroxenites from the Cabo Ortegal Complex, Spain. Journal of Petrology, 2016, 57, 1921-1954.	2.8	46
292	Mud Tank Zircon: Longâ€Term Evaluation of a Reference Material for Uâ€Pb Dating, Hfâ€Isotope Analysis and Trace Element Analysis. Geostandards and Geoanalytical Research, 2019, 43, 339-354.	3.1	46
293	Proterozoic mantle lithosphere beneath the extended margin of the South China block: In situ Re-Os evidence. Geology, 2003, 31, 709.	4.4	45
294	Super-reduced mineral assemblages in "ophiolitic" chromitites and peridotites: the view from Mount Carmel. European Journal of Mineralogy, 2017, 29, 557-570.	1.3	45
295	Super-reducing conditions in ancient and modern volcanic systems: sources and behaviour of carbon-rich fluids in the lithospheric mantle. Mineralogy and Petrology, 2018, 112, 101-114.	1.1	45
296	High- and low-Cr chromitite and dunite in a Tibetan ophiolite: evolution from mature subduction system to incipient forearc in the Neo-Tethyan Ocean. Contributions To Mineralogy and Petrology, 2017, 172, 1.	3.1	44
297	Trace elements in tourmalines from massive sulfides deposits and tourmalinites; geochemical controls and exploration applications. Economic Geology, 1996, 91, 657-675.	3.8	43
298	Cretaceous thermo-chemical modification of the Kaapvaal cratonic lithosphere, South Africa. Lithos, 2009, 112, 886-895.	1.4	43
299	Messengers from the deep: Fossil wadsleyite-chromite microstructures from the Mantle Transition Zone. Scientific Reports, 2015, 5, 16484.	3.3	43
300	Sulfur isotope composition of metasomatised mantle xenoliths from the Bultfontein kimberlite (Kimberley, South Africa): Contribution from subducted sediments and the effect of sulfide alteration on S isotope systematics. Earth and Planetary Science Letters, 2016, 445, 114-124.	4.4	43
301	Building cratonic keels in Precambrian plate tectonics. Nature, 2020, 586, 395-401.	27.8	43
302	Garnet granulite and associated xenoliths in minette and serpentinite diatremes of the Colorado Plateau. Geology, 1979, 7, 483.	4.4	42
303	A geotherm and lithospheric section for central Mongolia (Tariat region). Geodynamic Series, 1998, , 127-153.	0.1	42
304	Ultramafic Xenoliths from Kutch, Northwest India: Plume-Related Mantle Samples?. International Geology Review, 2000, 42, 416-444.	2.1	42
305	Chemical abrasion of zircon and ilmenite megacrysts in the Monastery kimberlite: Implications for the composition of kimberlite melts. Chemical Geology, 2014, 383, 76-85.	3.3	42

306 New data on lazurite. Lithos, 1976, 9, 39-54.

1.4 41

#	Article	IF	CITATIONS
307	The crust-mantle boundary beneath cratons and craton margins: a transect across the south-west margin of the Kaapvaal craton. Lithos, 1995, 36, 257-287.	1.4	41
308	Crustal evolution in the Georgetown Inlier, North Queensland, Australia: a detrital zircon grain study. Chemical Geology, 2007, 245, 198-218.	3.3	41
309	Ancient and juvenile components in the continental crust and mantle: Hf isotopes in zircon from Svecofennian magmatic rocks and rapakivi granites in Sweden. Lithosphere, 2011, 3, 409-419.	1.4	41
310	Gold in the mantle: A global assessment of abundance and redistribution processes. Lithos, 2018, 322, 376-391.	1.4	41
311	Lherzolite nodules from the Fen alkaline complex, Norway. Contributions To Mineralogy and Petrology, 1973, 38, 135-146.	3.1	40
312	Dating lower crust and upper mantle events: an ion microprobe study of xenoliths from kimberlitic pipes, South Australia. Lithos, 1994, 32, 77-94.	1.4	40
313	Fragments of ancient lunar crust: Petrology and geochemistry of ferroan noritic anorthosites from the Descartes region of the Moon. Geochimica Et Cosmochimica Acta, 1995, 59, 831-847.	3.9	40
314	Apatite halogens and Sr-O and zircon Hf-O isotopes: Recycled volatiles in Jurassic porphyry ore systems in southern Tibet. Chemical Geology, 2022, 605, 120924.	3.3	40
315	Parageneses of garnet in granulite-facies rocks, Lofoten-Vesteraalen, Norway. Contributions To Mineralogy and Petrology, 1969, 23, 89-116.	3.1	39
316	The thermal state and composition of the lithospheric mantle beneath the Leizhou Peninsula, South China. Journal of Volcanology and Geothermal Research, 2003, 122, 165-189.	2.1	39
317	Granulite xenoliths and their zircons, Tuoyun, NW China: Insights into southwestern Tianshan lower crust. Precambrian Research, 2006, 145, 159-181.	2.7	39
318	Os-isotope variability within sulfides from podiform chromitites. Chemical Geology, 2012, 291, 224-235.	3.3	39
319	Recycling of ancient subduction-modified mantle domains in the Purang ophiolite (southwestern) Tj ETQq1 1 0.7	784314 rg 1.4	BT /Overlock
320	Roles of Melting and Metasomatism in the Formation of the Lithospheric Mantle beneath the Leizhou Peninsula, South China. Journal of Petrology, 2006, 47, 355-383.	2.8	38
321	Zircon U–Pb ages and Hf–O isotopic composition of migmatites from the Zanjan–Takab complex, NW Iran: Constraints on partial melting of metasediments. Lithos, 2016, 240-243, 34-48.	1.4	38
322	Sr isotopic heterogeneity in primitive basaltic rocks, southeastern Australia: correlation with mantle metasomatism. Contributions To Mineralogy and Petrology, 1984, 87, 220-230.	3.1	37
323	Tracing the Caples Terrane through New Zealand using detrital zircon age patterns and radiogenic isotope signatures. New Zealand Journal of Geology, and Geophysics, 2009, 52, 223-245.	1.8	37
324	Persistence of mantle lithospheric Re–Os signature during asthenospherization of the subcontinental lithospheric mantle: insights from in situ isotopic analysis of sulfides from the Ronda peridotite (Southern Spain). Contributions To Mineralogy and Petrology, 2010, 159, 315-330.	3.1	37

#	Article	IF	CITATIONS
325	Heterogeneous sources of the Triassic granitoid plutons in the southern Qinling orogen: An Eâ€W tectonic division in central China. Tectonics, 2013, 32, 396-416.	2.8	37
326	Zircon U–Pb ages and Hf isotope of gneissic rocks from the Huai'an Complex: Implications for crustal accretion and tectonic evolution in the northern margin of the North China Craton. Precambrian Research, 2014, 255, 335-354.	2.7	37
327	Whitlockite and apatite from lunar rock 14310 and from×degården, Norway. Earth and Planetary Science Letters, 1972, 15, 53-58.	4.4	36
328	Origin and evolution of topaz-bearing granites from the Nanling Range, South China: a geochemical and Sr–Nd–Hf isotopic study. Mineralogy and Petrology, 2007, 90, 271-300.	1.1	36
329	A spectroscopic and carbon-isotope study of mixed-habit diamonds: Impurity characteristics and growth environment. American Mineralogist, 2013, 98, 66-77.	1.9	36
330	Formation of Eclogites and the Coronas in Anorthosites, Bergen Arcs, Norway. Memoir of the Geological Society of America, 1972, , 37-64.	0.5	35
331	Diamonds from Wellington, NSW: insights into the origin of eastern Australian diamonds. Mineralogical Magazine, 1999, 63, 447-471.	1.4	35
332	Platelet development in cuboid diamonds: insights from micro-FTIR mapping. Contributions To Mineralogy and Petrology, 2012, 164, 1011-1025.	3.1	35
333	Coupling, decoupling and metasomatism: Evolution of crust–mantle relationships beneath NW Spitsbergen. Lithos, 2012, 149, 115-135.	1.4	35
334	Petrology and geochemistry of peridotite xenoliths from the Lianshan region: Nature and evolution of lithospheric mantle beneath the lower Yangtze block. Gondwana Research, 2013, 23, 161-175.	6.0	35
335	Two″ayered oceanic lithospheric mantle in a <scp>T</scp> ibetan ophiolite produced by episodic subduction of <scp>T</scp> ethyan slabs. Geochemistry, Geophysics, Geosystems, 2017, 18, 1189-1213.	2.5	35
336	The Fen Damkjernite: Petrology of a "central-complex kimberlite― Physics and Chemistry of the Earth, 1975, 9, 163-177.	0.3	34
337	Petrogenesis of the Yangkou layered garnet-peridotite complex, Sulu UHP terrane, China. American Mineralogist, 2005, 90, 801-813.	1.9	34
338	The Kimberlites and related rocks of the Kuruman Kimberlite Province, Kaapvaal Craton, South Africa. Contributions To Mineralogy and Petrology, 2011, 161, 351-371.	3.1	34
339	In situ U–Pb Dating and Sr–Nd Isotopic Analysis of Perovskite: Constraints on the Age and Petrogenesis of the Kuruman Kimberlite Province, Kaapvaal Craton, South Africa. Journal of Petrology, 2012, 53, 2497-2522.	2.8	34
340	Metamorphism disturbs the Re-Os signatures of platinum-group minerals in ophiolite chromitites. Geology, 2012, 40, 659-662.	4.4	34
341	The architecture of the European-Mediterranean lithosphere: A synthesis of the Re-Os evidence. Geology, 2013, 41, 547-550.	4.4	34
342	From enriched to depleted mantle: Evidence from Cretaceous lamprophyres and Paleogene basaltic rocks in eastern and central Guangxi Province, western Cathaysia block of South China. Lithos, 2014, 184-187, 300-313.	1.4	34

#	Article	IF	CITATIONS
343	Trace-element geochemistry and U–Pb dating of perovskite in kimberlites of the Lunda Norte province (NE Angola): Petrogenetic and tectonic implications. Chemical Geology, 2016, 426, 118-134.	3.3	34
344	Abundances of K, Rb, Sr and Ba in some ultramafic rocks and minerals. Earth and Planetary Science Letters, 1968, 4, 497-501.	4.4	33
345	Morphology and geochemistry of zircons from late Mesozoic igneous complexes in coastal SE China: implications for petrogenesis. Mineralogical Magazine, 2002, 66, 235-251.	1.4	33
346	Mantle melts, metasomatism and diamond formation: Insights from melt inclusions in xenoliths from Diavik, Slave Craton. Lithos, 2009, 112, 675-682.	1.4	33
347	Zircon U-Pb and Hf isotopes of volcanic rocks from the Batamayineishan Formation in the eastern Junggar Basin. Science Bulletin, 2010, 55, 4150-4161.	1.7	33
348	The mid-Cretaceous transition from basement to cover within sedimentary rocks in eastern New Zealand: evidence from detrital zircon age patterns. Geological Magazine, 2013, 150, 455-478.	1.5	33
349	Episodic refertilization and metasomatism of Archean mantle: evidence from an orogenic peridotite in North Qaidam (NE Tibet, China). Contributions To Mineralogy and Petrology, 2015, 169, 1.	3.1	33
350	Detrital zircon ages in Buller and Takaka terranes, New Zealand: constraints on early Zealandia history. New Zealand Journal of Geology, and Geophysics, 2015, 58, 176-201.	1.8	33
351	Subduction, highâ€P metamorphism, and collision fingerprints in South Iran: Constraints from zircon Uâ€Pb and mica Rbâ€&r geochronology. Geochemistry, Geophysics, Geosystems, 2017, 18, 306-332.	2.5	33
352	Neoproterozoic sedimentary rocks track the location of the Lhasa Block during the Rodinia breakup. Precambrian Research, 2019, 320, 63-77.	2.7	33
353	Distribution of high field strength and rare earth elements in mantle and lower crustal xenoliths from the Southwestern United States: The role of grain-boundary phases. Geochimica Et Cosmochimica Acta, 2004, 68, 3919-3942.	3.9	32
354	The Gurupi Belt, northern Brazil: Lithostratigraphy, geochronology, and geodynamic evolution. Precambrian Research, 2005, 141, 83-105.	2.7	32
355	U–Pb and Hf-isotope analyses of zircon from the Kundelungu Kimberlites, D.R. Congo: Implications for crustal evolution. Precambrian Research, 2007, 156, 195-225.	2.7	32
356	MINERALOGY AND GEOCHEMISTRY OF PLATINUM-RICH CHROMITITES FROM THE MANTLE-CRUST TRANSITION ZONE AT OUEN ISLAND, NEW CALEDONIA OPHIOLITE. Canadian Mineralogist, 2011, 49, 1549-1569.	1.0	32
357	High-pressure experiments provide insights into the Mantle Transition Zone history of chromitite in Tibetan ophiolites. Earth and Planetary Science Letters, 2017, 463, 151-158.	4.4	32
358	<scp>GZ</scp> 7 and <scp>GZ</scp> 8 – Two Zircon Reference Materials for <scp>SIMS</scp> Uâ€₽b Geochronology. Geostandards and Geoanalytical Research, 2018, 42, 431-457.	3.1	32
359	A terrestrial magmatic hibonite-grossite-vanadium assemblage: Desilication and extreme reduction in a volcanic plumbing system, Mount Carmel, Israel. American Mineralogist, 2019, 104, 207-219.	1.9	32
360	Repeated magmatic buildup and deep "hot zones―in continental evolution: The Cadomian crust of Iran. Earth and Planetary Science Letters, 2020, 531, 115989.	4.4	32

#	Article	IF	CITATIONS
361	The granulite to eclogite transition beneath the eastern margin of the Australian craton. European Journal of Mineralogy, 1991, 3, 293-322.	1.3	32
362	The lower crust in eastern Australia: xenolith evidence. Geological Society Special Publication, 1986, 24, 363-374.	1.3	31
363	The lithospheric mantle beneath the southwestern Tianshan area, northwest China. Contributions To Mineralogy and Petrology, 2006, 151, 457-479.	3.1	31
364	Microinclusions in monocrystalline octahedral diamonds and coated diamonds from Diavik, Slave Craton: Clues to diamond genesis. Lithos, 2009, 112, 724-735.	1.4	31
365	Evolution of the Lüliangshan garnet peridotites in the North Qaidam UHP belt, Northern Tibetan Plateau: Constraints from Re–Os isotopes. Lithos, 2010, 117, 307-321.	1.4	31
366	Archean lithospheric mantle beneath Arkansas: Continental growth by microcontinent accretion. Bulletin of the Geological Society of America, 2011, 123, 1763-1775.	3.3	31
367	Coexistence of the moderately refractory and fertile mantle beneath the eastern Central Asian Orogenic Belt. Gondwana Research, 2013, 23, 176-189.	6.0	31
368	Diamond formation during metasomatism of mantle eclogite by chloride-carbonate melt. Contributions To Mineralogy and Petrology, 2018, 173, 1.	3.1	31
369	Lapis lazuli from Baffin island â \in " a precambrian meta-evaporite. Lithos, 1978, 11, 37-60.	1.4	30
370	Crustal zircons and mantle sulfides: Archean to Triassic events in the lithosphere beneath south-eastern Sicily. Lithos, 2007, 96, 503-523.	1.4	30
371	Deep earth recycling in the Hadean and constraints on surface tectonics. Numerische Mathematik, 2013, 313, 912-932.	1.4	30
372	Significance of ancient sulfide PGE and Re–Os signatures in the mantle beneath Calatrava, Central Spain. Contributions To Mineralogy and Petrology, 2014, 168, 1.	3.1	30
373	Fluid-present deformation aids chemical modification of chromite: Insights from chromites from Golyamo Kamenyane, SE Bulgaria. Lithos, 2015, 228-229, 78-89.	1.4	30
374	Subduction-related middle Permian to early Triassic magmatism in central Hainan Island, South China. Lithos, 2018, 318-319, 158-175.	1.4	30
375	Trace-element geochemistry of diamondite: Crystallisation of diamond from kimberlite–carbonatite melts. Lithos, 2008, 106, 39-54.	1.4	29
376	Major transformations reveal Earth's deep secrets. Geology, 2008, 36, 95.	4.4	29
377	Quantitative characterization of plastic deformation of single diamond crystals: A high pressure high temperature (HPHT) experimental deformation study combined with electron backscatter diffraction (EBSD). Diamond and Related Materials, 2012, 30, 20-30.	3.9	29
378	Trace element partitioning in mixed-habit diamonds. Chemical Geology, 2013, 355, 134-143.	3.3	29

#	Article	IF	CITATIONS
379	Pressure―and stressâ€induced fabric transition in olivine from peridotites in the Western Gneiss Region (Norway): implications for mantle seismic anisotropy. Journal of Metamorphic Geology, 2013, 31, 93-111.	3.4	29

Transfer of Os isotopic signatures from peridotite to chromitite in the subcontinental mantle: Insights from in situ analysis of platinum-group and base-metal minerals (Ojén peridotite massif,) Tj ETQq0 0 0 rgB4 /Overlæk 10 Tf 50

381	Evolution of coronas in Norwegian anorthosites: re-evaluation based on crystal-chemistry and microstructures. Contributions To Mineralogy and Petrology, 1985, 91, 330-339.	3.1	28
382	Lithospheric mantle structure and the diamond potential of kimberlites in southern D.R. Congo. Lithos, 2009, 112, 166-176.	1.4	28
383	Thermal metamorphism of mantle chromites and the stability of noble-metal nanoparticles. Contributions To Mineralogy and Petrology, 2015, 170, 1.	3.1	28
384	Trace-element fingerprints of chromite, magnetite and sulfides from the 3.1ÂGa ultramafic–mafic rocks of the Nuggihalli greenstone belt, Western Dharwar craton (India). Contributions To Mineralogy and Petrology, 2015, 169, 1.	3.1	28
385	Tectonothermal evolution of the continental crust beneath the Yakutian diamondiferous province (Siberian craton): U–Pb and Hf isotopic evidence on zircons from crustal xenoliths of kimberlite pipes. Precambrian Research, 2016, 282, 1-20.	2.7	28
386	How did the Dabie Orogen collapse? Insights from 3â€Ð magnetotelluric imaging of profile data. Journal of Geophysical Research: Solid Earth, 2016, 121, 5169-5185.	3.4	28
387	The recycling of chromitites in ophiolites from southwestern North America. Lithos, 2017, 294-295, 53-72.	1.4	28
388	Basement components of the Xiangshan-Yuhuashan area, South China: Defining the boundary between the Yangtze and Cathaysia blocks. Precambrian Research, 2018, 309, 102-122.	2.7	28
389	Unusual mineral inclusions and carbon isotopes of alluvial diamonds from Bingara, eastern Australia. Lithos, 2003, 69, 51-66.	1.4	27
390	Kimberlitic sources of super-deep diamonds in the Juina area, Mato Grosso State, Brazil. Lithos, 2010, 114, 16-29.	1.4	27
391	Laurentian Provenance of Archean Mantle Fragments in the Proterozoic Baltic Crust of the Norwegian Caledonides. Journal of Petrology, 2012, 53, 1357-1383.	2.8	27
392	Ages, trace elements and Hf-isotopic compositions of zircons from claystones around the Permian-Triassic boundary in the Zunyi Section, South China: Implications for nature and tectonic setting of the volcanism. Journal of Earth Science (Wuhan, China), 2015, 26, 872-882.	3.2	27
393	Lithological and age structure of the lower crust beneath the northern edge of the North China Craton: Xenolith evidence. Lithos, 2015, 216-217, 211-223.	1.4	27

Various growth environments of cloudy diamonds from the Malobotuobia kimberlite field (Siberian) Tj ETQq0 0 0 rgBT /Overlock 10 Tf 5

395	Cr-rich rutile: A powerful tool for diamond exploration. Lithos, 2016, 265, 304-311.	1.4	27
396	Detrital zircon geochronology and sandstone provenance of basement Waipapa Terrane (Triassic–Cretaceous) and Cretaceous cover rocks (Northland Allochthon and Houhora Complex) in northern North Island, New Zealand. Geological Magazine, 2013, 150, 89-109.	1.5	26

#	Article	IF	CITATIONS
397	Compositional effects on the solubility of minor and trace elements in oxide spinel minerals: Insights from crystal-crystal partition coefficients in chromite exsolution. American Mineralogist, 2016, 101, 1360-1372.	1.9	26
398	Zircon recycling and crystallization during formation of chromite- and Ni-arsenide ores in the subcontinental lithospheric mantle (SerranÃa de Ronda, Spain). Ore Geology Reviews, 2017, 90, 193-209.	2.7	26
399	East Antarctic sources of extensive Lower–Middle Ordovician turbidites in the Lachlan Orogen, southern Tasmanides, eastern Australia. Australian Journal of Earth Sciences, 2017, 64, 143-224.	1.0	26
400	Across-arc geochemical variations in the Paleogene magmatic belt of Iran. Lithos, 2019, 344-345, 280-296.	1.4	26
401	Application of the proton microprobe in mineral exploration and processing. Nuclear Instruments & Methods in Physics Research B, 1989, 40-41, 690-697.	1.4	25
402	The Belomorian eclogite province: Unique evidence of Meso-Neoarchaean subduction and collision. Doklady Earth Sciences, 2010, 434, 1311-1316.	0.7	25
403	Perspectives on Cretaceous Gondwana break-up from detrital zircon provenance of southern Zealandia sandstones. Geological Magazine, 2017, 154, 661-682.	1.5	25
404	Sources and timing of pyroxenite formation in the sub-arc mantle: Case study of the Cabo Ortegal Complex, Spain. Earth and Planetary Science Letters, 2017, 474, 490-502.	4.4	25
405	The Paleoproterozoic Vishnu basin in southwestern Laurentia: Implications for supercontinent reconstructions, crustal growth, and the origin of the Mojave crustal province. Precambrian Research, 2018, 308, 1-17.	2.7	25
406	Component variation in the late Neoproterozoic to Cambrian sedimentary rocks of SW China – NE Vietnam, and its tectonic significance. Precambrian Research, 2018, 308, 92-110.	2.7	25
407	Carmeltazite, ZrAl2Ti4O11, a New Mineral Trapped in Corundum from Volcanic Rocks of Mt Carmel, Northern Israel. Minerals (Basel, Switzerland), 2018, 8, 601.	2.0	25
408	Mantle-derived sapphirine. Mineralogical Magazine, 1986, 50, 635-640.	1.4	25
409	Evolution of Phanerozoic Eastern Australian Lithosphere: Isotopic Evidence for Magmatic and Tectonic Underplating. Journal of Petrology, 1988, Special_Volume, 89-108.	2.8	24
410	Nitrogen aggregation in metamorphic diamonds from Kazakhstan. Geochimica Et Cosmochimica Acta, 1994, 58, 5173-5177.	3.9	24
411	Statistical techniques for the classification of chromites in diamond exploration samples. Journal of Geochemical Exploration, 1997, 59, 233-249.	3.2	24
412	Distribution and characteristics of diamonds from Myanmar. Journal of Asian Earth Sciences, 2001, 19, 563-577.	2.3	24
413	Different styles of modern and ancient non-collisional orogens and implications for crustal growth: a Gondwanaland perspective. Canadian Journal of Earth Sciences, 2016, 53, 1372-1415.	1.3	24
414	Deformation of mantle pyroxenites provides clues to geodynamic processes in subduction zones: Case study of the Cabo Ortegal Complex, Spain. Earth and Planetary Science Letters, 2017, 472, 174-185.	4.4	24

#	Article	IF	CITATIONS
415	Generation of continental adakitic rocks: Crystallization modeling with variable bulk partition coefficients. Lithos, 2017, 272-273, 222-231.	1.4	24

Multi-stage modification of Paleoarchean crust beneath the Anabar tectonic province (Siberian) Tj ETQq0 0 0 rgBT $\frac{10}{2.7}$ verlock 10 Tf 50 70 $\frac{10}{2.7}$

417	Hf isotope composition of zircons and implication for the petrogenesis of Yajiangqiao granite, Hunan Province, China. Science Bulletin, 2003, 48, 995-998.	1.7	23
418	Mineral chemistry and zircon geochronology of xenocrysts and altered mantle and crustal xenoliths from the Aries micaceous kimberlite: Constraints on the composition and age of the central Kimberley Craton, Western Australia. Lithos, 2007, 93, 175-198.	1.4	23
419	Petrogenesis of eclogites enclosed in mantle-derived peridotites from the Sulu UHP terrane: constraints from trace elements in minerals and Hf isotopes in zircon. Lithos, 2009, 109, 176-192.	1.4	23
420	Provenance comparisons between the Nambucca Block, Eastern Australia and the Torlesse Composite Terrane, New Zealand: connections and implications from detrital zircon age patterns. Australian Journal of Earth Sciences, 2013, 60, 241-253.	1.0	23
421	Multiple Metasomatism beneath the Nógrád–Gömör Volcanic Field (Northern Pannonian Basin) Revealed by Upper Mantle Peridotite Xenoliths. Journal of Petrology, 2017, 58, 1107-1144.	2.8	23
422	Cold plumes trigger contamination of oceanic mantle wedges with continental crust-derived sediments: Evidence from chromitite zircon grains of eastern Cuban ophiolites. Geoscience Frontiers, 2018, 9, 1921-1936.	8.4	23
423	Late Cretaceous subduction-related magmatism on the southern edge of Sabzevar basin, NE Iran. Journal of the Geological Society, 2019, 176, 530-552.	2.1	23
424	Replacement antiperthites in gneisses of the Babbitt-Embarrass area, Minnesota, U. S. A Lithos, 1969, 2, 171-186.	1.4	22
425	Moho and petrologic crust-mantle boundary coincide under southeastern Australia: Comment and Reply. Geology, 1994, 22, 666.	4.4	22
426	The CSIRO-GEMOC Nuclear Microprobe: a high-performance system based on a new closely integrated design. Nuclear Instruments & Methods in Physics Research B, 1999, 158, 18-23.	1.4	22
427	Sulfides and chalcophile elements in Roberts Victor eclogites: Unravelling a sulfide-rich metasomatic event. Chemical Geology, 2013, 354, 73-92.	3.3	22
428	Unmasking xenolithic eclogites: Progressive metasomatism of a key Roberts Victor sample. Chemical Geology, 2014, 364, 56-65.	3.3	22
429	Recurrent magmatic activity on a lithosphere-scale structure: Crystallization and deformation in kimberlitic zircons. Gondwana Research, 2017, 42, 126-132.	6.0	22
430	Magma sources and gold mineralisation in the Mount Leyshon and Tuckers Igneous Complexes, Queensland, Australia: U-Pb and Hf isotope evidence. Lithos, 2008, 101, 281-307.	1.4	21
431	Hafnium-neodymium constraints on source heterogeneity of the economic ultramafic-mafic Noril'sk-1 intrusion (Russia). Lithos, 2013, 164-167, 36-46.	1.4	21
432	Sulfide metasomatism and the mobility of gold in the lithospheric mantle. Chemical Geology, 2015, 410, 149-161.	3.3	21

#	Article	IF	CITATIONS
433	Identification of Eocene-Oligocene magmatic pulses associated with flare-up in east Iran: Timing and sources. Gondwana Research, 2018, 57, 141-156.	6.0	21
434	Tectonic Switching of Southeast China in the Late Paleozoic. Journal of Geophysical Research: Solid Earth, 2018, 123, 8508-8526.	3.4	21
435	Langshan basalts record recycled Paleo-Asian oceanic materials beneath the northwest North China Craton. Chemical Geology, 2019, 524, 88-103.	3.3	21
436	Metamorphic feldspathization of metavolcanics and granitoids, Avnik area, Turkey. Contributions To Mineralogy and Petrology, 1983, 83, 309-319.	3.1	20
437	Multiple Origins of Alluvial Diamonds from New South Wales, Australia. Economic Geology, 2002, 97, 109-123.	3.8	20
438	Autochthonous inheritance of zircon through Cretaceous partial melting of Carboniferous plutons: the Arthur River Complex, Fiordland, New Zealand. Contributions To Mineralogy and Petrology, 2011, 161, 401-421.	3.1	20
439	Extreme lithium isotopic fractionation in three zircon standards (Plešovice, Qinghu and Temora). Scientific Reports, 2015, 5, 16878.	3.3	20
440	Sources of the Nanwenhe - Song Chay granitic complex (SW China - NE Vietnam) and its tectonic significance. Lithos, 2017, 290-291, 76-93.	1.4	20
441	Synthesis of inverse ringwoodite sheds light on the subduction history of Tibetan ophiolites. Scientific Reports, 2018, 8, 5457.	3.3	20
442	Extremely low structural hydroxyl contents in upper mantle xenoliths from the Nógrád-Gömör Volcanic Field (northern Pannonian Basin): Geodynamic implications and the role of post-eruptive re-equilibration. Chemical Geology, 2019, 507, 23-41.	3.3	20
443	Trace element composition of anorthosite plagioclase. Earth and Planetary Science Letters, 1974, 24, 213-223.	4.4	19
444	Lithospheric domains and controls on kimberlite emplacement, Slave Province, Canada: Evidence from elastic thickness and upper mantle composition. Geochemistry, Geophysics, Geosystems, 2005, 6, n/a-n/a.	2.5	19
445	Thallium isotopes as a potential tracer for the origin of cratonic eclogites. Geochimica Et Cosmochimica Acta, 2009, 73, 7387-7398.	3.9	19
446	Complex Precambrian crustal evolution beneath the northeastern Yangtze Craton reflected by zircons from Mesozoic volcanic rocks of the Fanchang basin, Anhui Province. Precambrian Research, 2012, 220-221, 91-106.	2.7	19
447	Water contents of Roberts Victor xenolithic eclogites: primary and metasomatic controls. Contributions To Mineralogy and Petrology, 2014, 168, 1.	3.1	19
448	Mid-Cretaceous lamproite from the Kutch region, Gujarat, India: Genesis and tectonic implications. Gondwana Research, 2014, 26, 942-956.	6.0	19
449	Microscale effects of melt infiltration into the lithospheric mantle: Peridotite xenoliths from Xilong, South China. Lithos, 2015, 232, 111-123.	1.4	19
450	An imbricate midcrustal suture zone: The Mojave-Yavapai Province boundary in Grand Canyon, Arizona. Bulletin of the Geological Society of America, 2015, 127, 1391-1410.	3.3	19

#	Article	IF	CITATIONS
451	Sulfide in dunite channels reflects long-distance reactive migration of mid-ocean-ridge melts from mantle source to crust: A Re-Os isotopic perspective. Earth and Planetary Science Letters, 2020, 531, 115969.	4.4	19
452	KRb fractionation by plagioclase feldspars. Chemical Geology, 1970, 6, 265-271.	3.3	18
453	The proton microprobe: a revolution in mineral analysis. Nuclear Instruments & Methods in Physics Research B, 1991, 54, 284-291.	1.4	18
454	Combined U-Pb dating and Sm-Nd studies on lower crustal and mantle xenoliths from the Delegate basaltic pipes, southeastern Australia. Contributions To Mineralogy and Petrology, 1998, 130, 154-161.	3.1	18
455	Tectonic affinities of the Houghton Inlier, South Australia: U–ÂPb and Hf-isotope data from zircons in modern stream sediments. Australian Journal of Earth Sciences, 2006, 53, 971-989.	1.0	18
456	Chapter 8.2 The Earliest Subcontinental Lithospheric Mantle. Neoproterozoic-Cambrian Tectonics, Global Change and Evolution: A Focus on South Western Gondwana, 2007, 15, 1013-1035.	0.2	18
457	Recognition of the Kaweka Terrane in northern South Island, New Zealand: preliminary evidence from Rb–Sr metamorphic and U–Pb detrital zircon ages. New Zealand Journal of Geology, and Geophysics, 2011, 54, 291-309.	1.8	18
458	Magnesium and oxygen isotopes in Roberts Victor eclogites. Chemical Geology, 2016, 438, 73-83.	3.3	18
459	Use and misuse of Mg- and Mn-rich ilmenite in diamond exploration: A petrographic and trace element approach. Lithos, 2017, 292-293, 348-363.	1.4	18
460	Spongy texture in mantle clinopyroxene recordsdecompression-induced melting. Lithos, 2018, 320-321, 144-154.	1.4	18
461	Unexposed Archean components and complex post-Archean accretion/reworking processes beneath the southern Yangtze Block revealed by zircon xenocrysts from the Paleozoic lamproites, South China. Precambrian Research, 2018, 316, 174-196.	2.7	18
462	Fluid inclusion studies of the Drammen Granite, Oslo Paleorift, Norway. Contributions To Mineralogy and Petrology, 1984, 87, 1-14.	3.1	17
463	An experimental calibration of the "nickel in garnet" geothermometer with applications, by D. Canil: discussion. Contributions To Mineralogy and Petrology, 1996, 124, 216-218.	3.1	17
464	Hf–Nd isotope constraints on the origin of Dehshir Ophiolite, Central Iran. Island Arc, 2012, 21, 202-214.	1.1	17
465	Nitrogen nanoinclusions in milky diamonds from Juina area, Mato Grosso State, Brazil. Lithos, 2016, 265, 57-67.	1.4	17
466	Widespread Paleoproterozoic basement in the eastern Cathaysia Block: Evidence from metasedimentary rocks of the Pingtan–Dongshan metamorphic belt, in southeastern China. Precambrian Research, 2016, 285, 91-108.	2.7	17
467	High-Mg adakitic rocks and their complementary cumulates formed by crystal fractionation of hydrous mafic magmas in a continental crustal magma chamber. Lithos, 2016, 260, 211-224.	1.4	17
468	Tracing ancient events in the lithospheric mantle: A case study from ophiolitic chromitites of SW Turkey. Journal of Asian Earth Sciences, 2016, 119, 1-19.	2.3	17

#	Article	IF	CITATIONS
469	Laurite and zircon from the Finero chromitites (Italy): New insights into evolution of the subcontinental mantle. Ore Geology Reviews, 2017, 90, 210-225.	2.7	17
470	Characterisation of primary and secondary carbonates in hypabyssal kimberlites: an integrated compositional and Sr-isotopic approach. Mineralogy and Petrology, 2018, 112, 555-567.	1.1	17
471	Permian to quaternary magmatism beneath the Mt Carmel area, Israel: Zircons from volcanic rocks and associated alluvial deposits. Lithos, 2018, 314-315, 307-322.	1.4	17
472	Late Paleocene adakitic granitoid from NW Iran and comparison with adakites in the NE Turkey: Adakitic melt generation in normal continental crust. Lithos, 2019, 346-347, 105151.	1.4	17
473	Mantle-like oxygen isotopes in kimberlites determined by in situ SIMS analyses of zoned olivine. Geochimica Et Cosmochimica Acta, 2019, 266, 274-291.	3.9	17
474	Early Paleozoic magmatism in northern Kontum Massif, Central Vietnam: Insights into tectonic evolution of the eastern Indochina Block. Lithos, 2020, 376-377, 105750.	1.4	17
475	Extreme reduction: Mantle-derived oxide xenoliths from a hydrogen-rich environment. Lithos, 2020, 358-359, 105404.	1.4	17
476	Isotopic microanalysis of seawater strontium in biogenic calcite to assess subsequent rehomogenisation during metamorphism. Chemical Geology, 2005, 220, 67-82.	3.3	16
477	The Salma Eclogites of the Belomorian Province, Russia. , 2011, , 623-670.		16
478	Microcontinents among the accretionary complexes of the Central Asia Orogenic Belt: In situ Re–Os evidence. Journal of Asian Earth Sciences, 2013, 62, 37-50.	2.3	16
479	Complex evolution of the lower crust beneath the southeastern North China Craton: the Junan xenoliths and xenocrysts. Lithos, 2014, 206-207, 113-126.	1.4	16
480	Inclusions of crichtonite-group minerals in Cr-pyropes from the Internatsionalnaya kimberlite pipe, Siberian Craton: Crystal chemistry, parageneses and relationships to mantle metasomatism. Lithos, 2018, 308-309, 181-195.	1.4	16
481	Insights into the mantle geochemistry of scandium from a meta-analysis of garnet data. Lithos, 2018, 310-311, 409-421.	1.4	16
482	Tracking Deep Lithospheric Events with Garnet-Websterite Xenoliths from Southeastern Australia. Journal of Petrology, 2018, 59, 901-930.	2.8	16
483	Cadomian Magmatic Rocks from Zarand (SE Iran) Formed in a Retro-Arc Basin. Lithos, 2020, 366-367, 105569.	1.4	16
484	Characterization of the metasomatic agent in mantle xenoliths from Devès, Massif Central (France) using coupled in situ trace-element and O, Sr and Nd isotopic compositions. Geological Society Special Publication, 2008, 293, 177-196.	1.3	15
485	Two stages of zircon crystallization in the Jingshan monzogranite, Bengbu Uplift: Implications for the syn-collisional granites of the Dabie–Sulu UHP orogenic belt and the climax of movement on the Tan-Lu fault. Lithos, 2011, 122, 201-213.	1.4	15
486	Nitrogen isotope systematics and origins of mixed-habit diamonds. Geochimica Et Cosmochimica Acta, 2015, 157, 1-12.	3.9	15

#	Article	IF	CITATIONS
487	Pre-Mesozoic Crimea as a continuation of the Dobrogea platform: insights from detrital zircons in Upper Jurassic conglomerates, Mountainous Crimea. International Journal of Earth Sciences, 2019, 108, 2407-2428.	1.8	15

Discussion of "Enigmatic super-reduced phases in corundum from natural rocks: Possible contamination from artificial abrasive materials or metallurgical slags―by Litasov etÂal. (Lithos,) Tj ETQq000 rgB1./Dverloct

489	A reappraisal of the metamorphic history of the Tehuitzingo chromitite, Puebla state, Mexico. International Geology Review, 2019, 61, 1706-1727.	2.1	15
490	Parageneses of TiB2 in corundum xenoliths from Mt. Carmel, Israel: Siderophile behavior of boron under reducing conditions. American Mineralogist, 2020, 105, 1609-1621.	1.9	15
491	Reconstructing the Source and Growth of the Makran Accretionary Complex: Constraints From Detrital Zircon Uâ€Pb Geochronology. Tectonics, 2020, 39, e2019TC005963.	2.8	15
492	Prolonged magmatism and growth of the Iran-Anatolia Cadomian continental arc segment in Northern Gondwana. Lithos, 2021, 384-385, 105940.	1.4	15
493	In-situ mineralogical interpretation of the mantle geophysical signature of the Gangdese Cu-porphyry mineral system. Gondwana Research, 2022, 111, 53-63.	6.0	15
494	Nuclear microprobe analysis of melt inclusions in minerals: Windows on metasomatic processes in the earth's mantle. Nuclear Instruments & Methods in Physics Research B, 2001, 181, 578-585.	1.4	14
495	Unusual Hf contents in metamorphic zircon from coesite-bearing eclogites of the Dabie Mountains, east-central China: implications for the dating of ultrahigh-pressure metamorphism. Journal of Metamorphic Geology, 2004, 22, 629-637.	3.4	14
496	Co-rich sulfides in mantle peridotites from Penghu Islands, Taiwan: Footprints of Proterozoic mantle plumes under the Cathaysia Block. Journal of Asian Earth Sciences, 2010, 37, 229-245.	2.3	14
497	Intrusion and contamination of high-temperature dunitic magma: the Nordre Bumandsfjord pluton, Seiland, Arctic Norway. Contributions To Mineralogy and Petrology, 2013, 165, 903-930.	3.1	14
498	Pink color in Type I diamonds: Is deformation twinning the cause?. American Mineralogist, 2015, 100, 1518-1527.	1.9	14
499	Nature and evolution of the lithospheric mantle beneath the eastern Central Asian Orogenic Belt: Constraints from peridotite xenoliths in the central part of the Great Xing'an Range, NE China. Lithos, 2015, 238, 52-63.	1.4	14
500	Gold in the mantle: The role of pyroxenites. Lithos, 2016, 244, 205-217.	1.4	14
501	An Australian provenance for the eastern Otago Schist protolith, South Island, New Zealand: evidence from detrital zircon age patterns and implications for the origin of its gold. Australian Journal of Earth Sciences, 2017, 64, 703-721.	1.0	14
502	Electrical structures in the northwest margin of the Junggar basin: Implications for its late Paleozoic geodynamics. Tectonophysics, 2017, 717, 473-483.	2.2	14
503	Discovery of the first natural hydride. American Mineralogist, 2019, 104, 611-614.	1.9	14
504	Similar crust beneath disrupted and intact cratons: Arguments against lower-crust delamination as a decratonization trigger. Tectonophysics, 2019, 750, 1-8.	2.2	14

#	Article	IF	CITATIONS
505	Perturbation of the deep-Earth carbon cycle in response to the Cambrian Explosion. Science Advances, 2022, 8, eabj1325.	10.3	14
506	Mineral reactions at a peridotite-gneiss contact, Jotunheimen, Norway. Mineralogical Magazine, 1971, 38, 435-445.	1.4	13
507	Trace element geochemistry of metabasalts from the KarmÃ,y ophiolite, southwest Norwegian Caledonides. Earth and Planetary Science Letters, 1980, 50, 75-91.	4.4	13
508	Calculation of equilibration conditions for garnet granulite and garnet websterite nodules in African kimberlite pipes. TMPM Tschermaks Mineralogische Und Petrographische Mitteilungen, 1981, 28, 229-244.	0.3	13
509	Upper mantle structure beneath eastern Siberia: Evidence from gravity modeling and mantle petrology. Geochemistry, Geophysics, Geosystems, 2003, 4, .	2.5	13
510	Petrology and Sr–Nd–Hf isotope geochemistry of gabbro xenoliths from the Hyblean Plateau: a MARID reservoir beneath SE Sicily?. Contributions To Mineralogy and Petrology, 2009, 157, 1-22.	3.1	13
511	Crustal structure of the Newer Volcanics Province, SE Australia, from ambient noise tomography. Tectonophysics, 2016, 683, 382-392.	2.2	13
512	Dellagiustaite: A Novel Natural Spinel Containing V2+. Minerals (Basel, Switzerland), 2019, 9, 4.	2.0	13
513	Metasomatic control of hydrogen contents in the layered cratonic mantle lithosphere sampled by Lac de Gras xenoliths in the central Slave craton, Canada. Geochimica Et Cosmochimica Acta, 2020, 286, 29-53.	3.9	13
514	Kishonite, VH2, and Oreillyite, Cr2N, Two New Minerals from the Corundum Xenocrysts of Mt Carmel, Northern Israel. Minerals (Basel, Switzerland), 2020, 10, 1118.	2.0	13
515	Collisionâ€related porphyry Cu deposits formed by input of ultrapotassic melts into the sulfideâ€rich lower crust. Terra Nova, 2021, 33, 582-589.	2.1	13
516	Immiscible metallic melts in the deep Earth: clues from moissanite (SiC) in volcanic rocks. Science Bulletin, 2020, 65, 1479-1488.	9.0	13
517	Rb-Sr geochronology of the Bitlis Massif, Avnik (Bingöl) area, S.E. Turkey. Geological Society Special Publication, 1984, 17, 403-413.	1.3	12
518	Applications of OlivineOrthopyroxeneSpinel Oxygen Geobarometers to the Redox State of the Upper Mantle. Journal of Petrology, 1991, Special_Volume, 291-306.	2.8	12
519	A cobalt-rich spinel inclusion in a sapphire from Bo Ploi, Thailand. Mineralogical Magazine, 1994, 58, 247-258.	1.4	12
520	Archean mantle contributes to the genesis of chromitite in the Palaeozoic Sartohay ophiolite, Asiatic Orogenic Belt, northwestern China. Precambrian Research, 2012, 216-219, 87-94.	2.7	12
521	Re-Os isotopic constraints on the evolution of the Bangong-Nujiang Tethyan oceanic mantle, Central Tibet. Lithos, 2015, 224-225, 32-45.	1.4	12
522	Eclogites in peridotite massifs in the Western Gneiss Region, Scandinavian Caledonides: Petrogenesis and comparison with those in the Variscan Moldanubian Zone. Lithos, 2018, 322, 325-346.	1.4	12

#	Article	IF	CITATIONS
523	Lateral and Vertical Heterogeneity in the Lithospheric Mantle at the Northern Margin of the Pannonian Basin Reconstructed From Peridotite Xenolith Microstructures. Journal of Geophysical Research: Solid Earth, 2019, 124, 6315-6336.	3.4	12
524	Lithospheric memory of subduction in mantle pyroxenite xenoliths from rift-related basalts. Earth and Planetary Science Letters, 2020, 544, 116365.	4.4	12
525	Are Xenoliths From Southwestern Kaapvaal Craton Representative of the Broader Mantle? Constraints From Magnetotelluric Modeling. Geophysical Research Letters, 2021, 48, e2021GL092570.	4.0	12
526	Geochemistry and Origin of Sulphide Minerals in Mantle Xenoliths: Qilin, Southeastern China. Journal of Petrology, 1999, 40, 1125-1149.	2.8	12
527	Thermochemical structure and evolution of cratonic lithosphere in central and southern Africa. Nature Geoscience, 2022, 15, 405-410.	12.9	12
528	In situ Re-Os isotope ages of sulfides in Hannuoba peridotitic xenoliths: Significance for the frequently-occurring mantle events beneath the North China Block. Science Bulletin, 2007, 52, 2847-2853.	1.7	11
529	Post-entrainment mineral-magma interaction in mantle xenoliths from inner Mongolia, western North China craton. Journal of Earth Science (Wuhan, China), 2012, 23, 54-76.	3.2	11
530	Sources of cratonic metasomatic fluids: In situ LA-MC-ICPMS analysis of Sr, Nd, Hf and Pb isotopes in Lima from the Jagersfontein Kimberlite. Numerische Mathematik, 2014, 314, 435-461.	1.4	11
531	Precambrian tectonic attribution and evolution of the Songliao terrane revealed by zircon xenocrysts from Cenozoic alkali basalts, Xilinhot region, NE China. Precambrian Research, 2014, 251, 33-48.	2.7	11
532	Phanerozoic magma underplating and crustal growth beneath the North China Craton. Terra Nova, 2017, 29, 211-217.	2.1	11
533	Formation of atoll garnets in the UHP eclogites of the Tso Morari Complex, Ladakh, Himalaya. Journal of Earth System Science, 2017, 126, 1.	1.3	11
534	Three types of element fluxes from metabasite into peridotite in analogue experiments: Insights into subduction-zone processes. Lithos, 2018, 302-303, 203-223.	1.4	11
535	Constraints from zircon Hf-O-Li isotopic compositions on the genesis of slightly low-δ18O alkaline granites in the Taohuadao area, Zhejiang Province, SE China. Journal of Asian Earth Sciences, 2018, 167, 197-208.	2.3	11
536	Titanates of the lindsleyite–mathiasite (LIMA) group reveal isotope disequilibrium associated with metasomatism in the mantle beneath Kimberley (South Africa). Earth and Planetary Science Letters, 2018, 482, 253-264.	4.4	11
537	New constraints on the source, composition, and post-emplacement modification of kimberlites from in situ C–O–Sr-isotope analyses of carbonates from the Benfontein sills (South Africa). Contributions To Mineralogy and Petrology, 2020, 175, 1.	3.1	11
538	Cr2O3 in corundum: Ultrahigh contents under reducing conditions. American Mineralogist, 2021, 106, 1420-1437.	1.9	11
539	Subduction initiation causes broad upper plate extension: The Late Cretaceous Iran example. Lithos, 2021, 398-399, 106296.	1.4	11
540	Comment on "Ultra-high pressure and ultra-reduced minerals in ophiolites may form by lightning strikes―by Ballhaus et al., 2017: Ultra-high pressure and super-reduced minerals in ophiolites do not form by lightning strikes. Geochemical Perspectives Letters, 0, , 1-2.	5.0	11

#	Article	IF	CITATIONS
541	Light oxygen isotopes in mantle-derived magmas reflect assimilation of sub-continental lithospheric mantle material. Nature Communications, 2021, 12, 6295.	12.8	11
542	IBA in minerals research: Progress and prospects. Nuclear Instruments & Methods in Physics Research B, 1990, 45, 604-609.	1.4	10
543	Heterogeneity in the thermal state of the lower crust and upper mantle beneath eastern Australia. Exploration Geophysics, 1991, 22, 295-298.	1.1	10
544	Deformation microstructures reveal a complex mantle history for polycrystalline diamond. Geochemistry, Geophysics, Geosystems, 2012, 13, .	2.5	10
545	Carboniferous and Permian granites of the northern Tasman orogenic belt, Queensland, Australia: insights into petrogenesis and crustal evolution from an in situ zircon study. International Journal of Earth Sciences, 2013, 102, 647-669.	1.8	10
546	Magnetic mineralogy of pyroxenite xenoliths from Hannuoba basalts, northern North China Craton: Implications for magnetism in the continental lower crust. Journal of Geophysical Research: Solid Earth, 2014, 119, 806-821.	3.4	10
547	Ancient mantle lithosphere beneath the Khanka massif in the Russian Far East: <i>inÂsitu</i> Re–Os evidence. Terra Nova, 2015, 27, 277-284.	2.1	10
548	Geochronology and geochemistry of deep-seated crustal xenoliths in the northern North China Craton: Implications for the evolution and structure of the lower crust. Lithos, 2017, 292-293, 1-14.	1.4	10
549	Carbon isotopes of eclogite-hosted diamonds from the Nyurbinskaya kimberlite pipe, Yakutia: The metasomatic origin of diamonds. Chemical Geology, 2017, 455, 131-147.	3.3	10
550	Hadean continental crust in the southern North China Craton: Evidence from the Xinyang felsic granulite xenoliths. Precambrian Research, 2018, 307, 155-174.	2.7	10
551	Siderophile and chalcophile elements in spinels, sulphides and native Ni in strongly metasomatised xenoliths from the Bultfontein kimberlite (South Africa). Lithos, 2021, 380-381, 105880.	1.4	10
552	Ti3+ in corundum traces crystal growth in a highly reduced magma. Scientific Reports, 2021, 11, 2439.	3.3	10
553	Deep lithosphere of the North China Craton archives the fate of the Paleo-Asian Ocean. Earth-Science Reviews, 2021, 215, 103554.	9.1	10
554	Immiscible metallic melts in the upper mantle beneath Mount Carmel, Israel: Silicides, phosphides, and carbides. American Mineralogist, 2022, 107, 532-549.	1.9	10
555	Melt Migration and Interaction in a Dunite Channel System within Oceanic Forearc Mantle: the Yushigou Harzburgite–Dunite Associations, North Qilian Ophiolite (NW China). Journal of Petrology, 2021, 62, .	2.8	10
556	Probing the Southern African Lithosphere With Magnetotellurics: 2. Linking Electrical Conductivity, Composition, and Tectonomagmatic Evolution. Journal of Geophysical Research: Solid Earth, 2022, 127,	3.4	10
557	Application of the proton microprobe to diamond exploration and genesis. Nuclear Instruments & Methods in Physics Research B, 1990, 49, 318-322.	1.4	9
558	The boundary phase and the melting of CaSiO 3 and MgSiO 3 perovskites. Journal of Physics and Chemistry of Solids, 2000, 61, 1815-1820.	4.0	9

#	Article	IF	CITATIONS
559	First isotopic data on detrital zircons from the Engane-Pe Uplift (western Polar Urals): Implications for the primary tectonic position of the Pre-Uralides-Timanides. Doklady Earth Sciences, 2009, 426, 567-573.	0.7	9
560	Rodinian detrital zircons in Late Cretaceous sandstones indicate a possible Precambrian basement under southern Zealandia. Precambrian Research, 2012, 212-213, 13-20.	2.7	9
561	Downward rejuvenation of the continental lower crust beneath the southeastern North China Craton. Tectonophysics, 2019, 750, 213-228.	2.2	9
562	Reworking of old continental lithosphere: Unradiogenic Os and decoupled Hf Nd isotopes in sub-arc mantle pyroxenites. Lithos, 2020, 354-355, 105346.	1.4	9
563	Diamond-forming HDFs tracking episodic mantle metasomatism beneath Nyurbinskaya kimberlite pipe (Siberian craton). Contributions To Mineralogy and Petrology, 2020, 175, 1.	3.1	9
564	The Paleogene ophiolite conundrum of the Iran–Iraq border region. Journal of the Geological Society, 2020, 177, 955-964.	2.1	9
565	Hidden Eoarchean crust in the southwestern Central Asian Orogenic Belt. Lithos, 2020, 360-361, 105437.	1.4	9
566	Pyroxenite Xenoliths Record Complex Melt Impregnation in the Deep Lithosphere of the Northwestern North China Craton. Journal of Petrology, 2021, 62, .	2.8	9
567	Fluid inclusion studies of the Drammen Granite, Oslo Paleorift, Norway. Contributions To Mineralogy and Petrology, 1984, 87, 15-23.	3.1	8
568	Mapping the Earth's mantle in 4D using the proton microprobe. Nuclear Instruments & Methods in Physics Research B, 1995, 104, 456-463.	1.4	8
569	Lithosphere structure and evolution in southeastern Australia. , 2003, , .		8
570	Detrital pyrope garnets from the El Kseibat area, Algeria: A glimpse into the lithospheric mantle beneath the north-eastern edge of the West African Craton. Journal of African Earth Sciences, 2012, 63, 1-11.	2.0	8
571	Magnetically stratified continental lower crust preserved in the North China Craton. Tectonophysics, 2015, 643, 73-79.	2.2	8
572	Re–Os isotopic constraints on the source of platinum-group minerals (PGMs) from the Vestřev pyrope-rich garnet placer deposit, Bohemian Massif. Ore Geology Reviews, 2015, 68, 117-126.	2.7	8
573	New Insights on the Origin of Ultramafic-Mafic Intrusions and Associated Ni-Cu-PGE Sulfide Deposits of the Noril'sk and Taimyr Provinces, Russia. , 2018, , 197-238.		8
574	Timing the tectonic mingling of ultramafic rocks and metasediments in the southern section of the coastal accretionary complex of central Chile. International Geology Review, 2018, 60, 2031-2045.	2.1	8
575	Geochronology and geochemistry of exotic blocks of Cadomian crust from the salt diapirs of SE Zagros: the Chah-Banu example. International Geology Review, 2022, 64, 1409-1430.	2.1	8
576	K/Rb in amphiboles and amphibolites from Northeastern Minnesota. Earth and Planetary Science Letters, 1967, 3, 367-370.	4.4	7

#	Article	IF	CITATIONS
577	DIAMOND FROM THE LOS COQUITOS AREA, BOLIVAR STATE, VENEZUELA. Canadian Mineralogist, 2006, 44, 323-340.	1.0	7
578	Temporal and genetic relationships between the Kidston gold-bearing Breccia Pipe and the Lochaber Ring Dyke Complex, North Queensland, Australia: insights from in situ U–Pb and Hf-isotope analysis of zircon. Mineralogy and Petrology, 2009, 95, 17-45.	1.1	7
579	Lithospheric mantle evolution beneath northeast Australia. Lithos, 2011, 125, 405-422.	1.4	7
580	Detrital zircon U-Pb age and Hf-isotope perspective on sediment provenance and tectonic models in SE Asia. , 2012, , .		7
581	Early Mesozoic deep-crust reworking beneath the central Lhasa terrane (South Tibet): Evidence from intermediate gneiss xenoliths in granites. Lithos, 2017, 274-275, 225-239.	1.4	7
582	Clobal- to Deposit-Scale Controls on Orthomagmatic Ni-Cu(-PGE) and PGE Reef Ore Formation. , 2018, , 1-46.		7
583	Melting Dynamics of Late Cretaceous Lamprophyres in Central Asia Suggest a Mechanism to Explain Many Continental Intraplate Basaltic Suite Magmatic Provinces. Journal of Geophysical Research: Solid Earth, 2021, 126, e2021JB021663.	3.4	7
584	Metamorphic history and Neoarchean–Paleoproterozoic crustal growth of the central Trans-North China Orogen: Evidence from granulite- to amphibolite-facies rocks of the Hengshan complex. Gondwana Research, 2021, 93, 162-183.	6.0	7
585	Decratonization and reactivation of the southern Indian shield: An integrated perspective. Earth-Science Reviews, 2021, 220, 103702.	9.1	7
586	Single zircon LAM-ICPMS U-Pb dating of Guidong complex (SE China) and its petrogenetic significance. Science Bulletin, 2003, 48, 1892.	1.7	7
587	Where did the Kontum Massif in central Vietnam come from?. Precambrian Research, 2022, 377, 106725.	2.7	7
588	Petrology, mineral chemistry, and exploration significance of Fe-sulfides from the metal dispersion halo surrounding the Cadjebut ZnPb MVT deposit, Western Australia. Applied Geochemistry, 1997, 12, 37-54.	3.0	6
589	Paleogeothermal gradients in Australia: Key to 4â€D lithosphere mapping*. Australian Journal of Earth Sciences, 1998, 45, 817-821.	1.0	6
590	Seeking the primary compositions of mantle xenoliths: Isotopic and elemental consequences of sequential leaching treatments on an eclogite suite. Chemical Geology, 2012, 328, 137-148.	3.3	6
591	Granulite facies xenoliths from the Yuhuashan complex, central Jiangxi, South China: constraints on Late Palaeozoic orogeny and middle″ower crust components. Journal of Metamorphic Geology, 2016, 34, 45-61.	3.4	6
592	An Orphaned Baltic Terrane in the Greenland Caledonides: A Sm-Nd and Detrital Zircon Study of a High-Pressure/Ultrahigh-Pressure Complex in Liverpool Land. Journal of Geology, 2016, 124, 541-567.	1.4	6
593	The Earliest Subcontinental Lithospheric Mantle. , 2019, , 81-102.		6
594	Re-Os Isotope Systematics of Sulfides in Chromitites and Host Lherzolites of the Andaman Ophiolite, India. Minerals (Basel, Switzerland), 2020, 10, 686.	2.0	6

#	Article	IF	CITATIONS
595	Oceanization of the subcontinental lithospheric mantle recorded in the Yunzhug ophiolite, Central Tibetan Plateau. Lithos, 2020, 370-371, 105612.	1.4	6
596	The Middle-Late Cretaceous Zagros ophiolites, Iran: Linking of a 3000 km swath of subduction initiation fore-arc lithosphere from Troodos, Cyprus to Oman. Bulletin of the Geological Society of America, 0, , .	3.3	6
597	Composition of diamond-forming media in cuboid diamonds from the V. Grib kimberlite pipe (Arkhangelsk province, Russia). Geochemical Journal, 2017, 51, 205-213.	1.0	6
598	Structure and composition of the lithosphere beneath Mount Carmel, North Israel. Contributions To Mineralogy and Petrology, 2022, 177, 1.	3.1	6
599	Variations of the Effective Elastic Thickness (Te) and Structure of the Lithosphere Beneath the Slave Province, Canada. Exploration Geophysics, 2005, 36, 266-271.	1.1	5
600	Zircon U-Pb dating and Lu-Hf isotope study of intermediate-mafic sub-volcanic and intrusive rocks in the Lishui Basin in the middle and lower reaches of Yangtze River. Science Bulletin, 2014, 59, 3427-3440.	1.7	5
601	Carbonate-silicate composition of diamond-forming media of fibrous diamonds from the Snap Lake area (Canada). Doklady Earth Sciences, 2015, 461, 297-300.	0.7	5
602	Deposits associated with ultramafic–mafic complexes in Mexico: the Loma Baya case. Ore Geology Reviews, 2017, 81, 1053-1065.	2.7	5
603	Chapter 14â€∫Crossing Cook Strait: terranes of the Marlborough Schist, Kapiti Island and Wellington. Geological Society Memoir, 2019, 49, 323-330.	1.7	5
604	Oxygen-Hafnium-Neodymium Isotope Constraints on the Origin of the Talnakh Ultramafic-Mafic Intrusion (Norilsk Province, Russia). Economic Geology, 2020, 115, 1195-1212.	3.8	5
605	Thermal architecture of cratonic India and implications for decratonization of the Western Dharwar Craton: Evidence from mantle xenoliths in the Deccan Traps. Lithos, 2021, 382-383, 105927.	1.4	5
606	Detrital zircon provenance of Permian to Triassic Gondwana sequences, Zealandia and eastern Australia. New Zealand Journal of Geology, and Geophysics, 2022, 65, 457-469.	1.8	5
607	Amphibolites from makran accretionary complex record Permian-Triassic Neo-Tethyan evolution. International Geology Review, 2022, 64, 1594-1610.	2.1	5
608	Diamonds from Myanmar and Thailand: Characteristics and Possible Origins. Economic Geology, 2001, 96, 0159-170.	3.8	5
609	Hf isotope composition of zircons and implication for the petrogenesis of Yajiangqiao granite, Hunan Province, China. Science Bulletin, 2003, 48, 995.	1.7	5
610	Depletion of the upper mantle by convergent tectonics in the Early Earth. Scientific Reports, 2021, 11, 21489.	3.3	5
611	Metasomatism versus host magma infiltration: A case study of Sal mantle xenoliths, Cape Verde Archipelago. , 2011, , .		4
612	Mechanical Mixing of Garnet Peridotite and Pyroxenite in the Orogenic Peridotite Lenses of the Tvaerdal Complex, Liverpool Land, Greenland Caledonides. Journal of Petrology, 2018, 59, 2191-2220.	2.8	4

#	Article	IF	CITATIONS
613	Nitrogen under Super-Reducing Conditions: Ti Oxynitride Melts in Xenolithic Corundum Aggregates from Mt Carmel (N. Israel). Minerals (Basel, Switzerland), 2021, 11, 780.	2.0	4
614	Linking ocean subduction with early Paleozoic intracontinental orogeny in South China: Insights from the Xiaying complex in eastern Guangxi Province. Lithos, 2021, 398-399, 106258.	1.4	4
615	Zn-, Mg- and O-isotope evidence for the origin of mantle eclogites from Roberts Victor kimberlite (Kaapvaal Craton, South Africa). Geology, 2022, 50, 593-597.	4.4	4
616	Trace element characteristics in the diopsides of peridotite xenoliths: a laser ablation-inductively coupled plasma-mass spectrometry study. Science Bulletin, 1998, 43, 579-583.	1.7	3
617	Petrography and Geochemistry of Peridotite Xenoliths from Hannuoba and Significance for Lithospheric Mantle Evolution. Journal of China University of Geosciences, 2006, 17, 25-33.	0.5	3
618	Zircon U-Pb, geochemical and isotopic constraints on the age and origin of A- and I-type granites and gabbro-diorites from NW Iran. Lithos, 2020, 374-375, 105688.	1.4	3
619	Detrital zircon age studies of Haast Schist in western Otago and Marlborough, New Zealand: constraints on their protolith age, terrane ancestry and Au–W mineralisation. Australian Journal of Earth Sciences, 2021, 68, 381-396.	1.0	3
620	Immiscible-melt inclusions in corundum megacrysts: Microanalyses and geological implications. American Mineralogist, 2021, 106, 559-569.	1.9	3
621	The microstructure of layered ultramafic cumulates: Case study of the Bear Creek intrusion, Trinity ophiolite, California, USA. Lithos, 2021, 388-389, 106047.	1.4	3
622	Proton-Microprobe Trace Element Study of Selected Leg 135 Core Samples. , 0, , .		3
623	Zircons from the Wambidgee Serpentinite Belt, southern Lachlan Orogen: evidence for oceanic crust at the Cambrian–Ordovician boundary. Australian Journal of Earth Sciences, 2022, 69, 406-418.	1.0	3
624	Geochemical and isotopic evolution of Late Oligocene magmatism in Quchan, NE Iran. Geochemistry, Geophysics, Geosystems, 2021, 22, e2021GC009973.	2.5	3
625	Open System Re-Os Isotope Behavior in Platinum-Group Minerals during Laterization?. Minerals (Basel,) Tj ETQq1	1 0.7843 2.0	14 ₃ rgBT /Ove
626	Discussion of â€~K/Rb in amphiboles and amphibolites from Northeastern Minnesota'. Earth and Planetary Science Letters, 1968, 4, 30-32.	4.4	2
627	Carbonatites at 200 km: quenched melt inclusions in megacrystalline Iherzolite xenoliths, Slave Craton, Canada. Journal of African Earth Sciences, 2001, 32, A35.	2.0	2
628	Upper mantle composition: Tools for smarter diamond exploration. , 2005, , 7-10.		2
629	Temporal correlation of magmatic-tectonic events in the lower and upper crust in north-east Australia. International Journal of Earth Sciences, 2012, 101, 1091-1109.	1.8	2
630	Characterization of the metasomatizing agent in the upper mantle beneath the northern Pannonian Basin based on Raman imaging, FIB-SEM, and LA-ICP-MS analyses of silicate melt inclusions in spinel peridotite. American Mineralogist, 2021, 106, 685-700.	1.9	2

William L. Griffin

#	Article	IF	CITATIONS
631	THE GREFSHEIM (NORWAY) METEORITE: A NEW L5 CHONDRITE. Meteoritics, 1979, 14, 117-120.	1.4	1
632	Diamond exploration and mantle structure imaging using PIXE microanalysis. Nuclear Instruments & Methods in Physics Research B, 1996, 109-110, 601-605.	1.4	1
633	Diamonds from Myanmar and Thailand: Characteristics andPossible Origins. Economic Geology, 2001, 96, 0159-170.	3.8	1
634	Granulite xenoliths from Cenozoic Basalts in SE China provide geochemical fingerprints to distinguish lower crust terranes from the North and South China tectonic blocks—Reply. Lithos, 2004, 73, 135-144.	1.4	1
635	Geochronology in New South Wales. Australian Journal of Earth Sciences, 2008, 55, 737-740.	1.0	1
636	Geoscience Data Integration: Insights into Mapping Lithospheric Architecture. ASEG Extended Abstracts, 2015, 2015, 1-2.	0.1	1
637	Complex evolution of the lower crust beneath the southeastern North China Craton: The Junan xenoliths and xenocrysts: Reply. Lithos, 2015, 234-235, 96-99.	1.4	1
638	Provenance of Jurassic sandstones in the Rakaia Terrane, Canterbury, New Zealand. New Zealand Journal of Geology, and Geophysics, 2018, 61, 136-144.	1.8	1
639	Making and unmaking continental mantle: Geochemical and geophysical perspectives. Acta Geologica Sinica, 2019, 93, 249-250.	1.4	1
640	Petrography and perovskite U-Pb age of the Katuba kimberlite, Kundelungu Plateau (D.R. Congo): Implications for regional tectonism and mineralisation. Journal of African Earth Sciences, 2019, 156, 35-43.	2.0	1
641	Phanerozoic orogeny in the South China Block traced by clastic components from Cambrian to Triassic sedimentary rocks. Journal of Asian Earth Sciences, 2021, 216, 104827.	2.3	1
642	THE FEN DAMKJERNITE: PETROLOGY OF A "CENTRAL-COMPLEX KIMBERLITEâ€, 1975, , 163-177.		1
643	Zircon xenocrysts in late cretaceous magmatic rocks in the kermanshah ophiolite: link to Iran continental crust supports the subduction initiation model. International Geology Review, 0, , 1-12.	2.1	1
644	Detrital zircons in Triassic–Cretaceous sandstones, Clarence-Moreton Basin, eastern Australia: speculations upon Australia and Zealandia provenances. Australian Journal of Earth Sciences, 2022, 69, 909-928.	1.0	1
645	Nordic carbonatite symposium — Alnö, 1979. Lithos, 1980, 13, 109.	1.4	Ο
646	Papers from SIEC. Lithos, 1986, 19, 169.	1.4	0
647	Ore deposits and the role of the lithospheric mantle. Lithos, 2013, 164-167, 1.	1.4	Ο
648	Reply to dunite magma or ultramafic cumulates? A discussion of Griffin et al. "Intrusion and contamination of high-temperature dunite magma: the Nordre Bumandsfjord pluton, Seiland, Arctic Norway― Contributions To Mineralogy and Petrology, 2013, 166, 1543-1544.	3.1	0

#	Article	IF	CITATIONS
649	Petrogenesis and geochronology of Cretaceous adakitic, I- and A-type granitoids in the NE Yangtze block: Constraints on the eastern subsurface boundary between the North and South China blocks: Reply. Lithos, 2014, 196-197, 380-383.	1.4	0
650	Chromium in Corundum: Ultra-high Contents Under Reducing Conditions. Microscopy and Microanalysis, 2019, 25, 2484-2485.	0.4	0
651	Reply to comment by Qi and Wang on "Similar crust beneath disrupted and intact cratons: Arguments against lower-crust delamination as a decratonization trigger― Tectonophysics, 2019, 767, 128156.	2.2	0
652	A Showcase of Analytical Techniques: Native V in Hibonite. Microscopy and Microanalysis, 2019, 25, 2486-2487.	0.4	0
653	Lithospheric mapping: a pathfinder for hidden terrane and ore systems in southren Lhasa block. Acta Geologica Sinica, 2019, 93, 204-204.	1.4	0
654	Emplacement age of the Tshibwe kimberlite, Democratic Republic of Congo, by in-situ LAM-ICPMS U/Pb dating of groundmass perovskite. Journal of African Earth Sciences, 2019, 157, 103502.	2.0	0
655	The integration of geophysics and geochemistry reveals the nature of the lithosphere beneath the Slave Craton (Canada). ASEG Extended Abstracts, 2004, 2004, 1-3.	0.1	0
656	The evolution of lithospheric domains: A new framework to enhance mineral exploration targeting. , 2005, , 41-44.		0